Technical Review

No. 1 · 1990

Gas Monitoring

Brüel & Kjær

Previously issued numbers of Brüel & Kjær Technical Review

2–1989 STSF – Practical instrumentation and application
Digital Filter Analysis: Real-time and Non Real-time Performance
1–1989 STSF – A Unique Technique for scan based Near-field Acoustic Holography without restrictions on coherence
2–1988 Quantifying Draught Risk
1–1988 Using Experimental Modal Analysis to Simulate Structural Dynamic Modifications
Use of Operational Deflection Shapes for Noise Control of Discrete Tones
4–1987 Windows to FFT Analysis (Part II).
Acoustic Calibrator for Intensity Measurement Systems
3–1987 Windows to FFT Analysis (Part I)
2–1987 Recent Developments in Accelerometer Design
Trends in Accelerometer Calibration
1–1987 Vibration Monitoring of Machines
4–1986 Field Measurements of Sound Insulation with a Battery-Operated Intensity Analyzer
Pressure Microphones for Intensity Measurements with Significantly Improved Phase Properties
Measurement of Acoustical Distance between Intensity Probe Microphones
Wind and Turbulence Noise of Turbulence Screen, Nose Cone and Sound Intensity Probe with Wind Screen
3–1986 A Method of Determining the Modal Frequencies of Structures with Coupled Modes
Improvement to Monoreference Modal Data by Adding an Oblique Degree of Freedom for the Reference
2–1986 Quality in Spectral Match of Photometric Transducers
Guide to Lighting of Urban Areas
1–1986 Environmental Noise Measurements
4–1985 Validity of Intensity Measurements in Partially Diffuse Sound Field
Influence of Tripods and Microphone Clips on the Frequency Response of Microphones
3–1985 The Modulation Transfer Function in Room Acoustics
RASTI: A Tool for Evaluating Auditoria
2–1985 Heat Stress
A New Thermal Anemometer Probe for Indoor Air Velocity Measurements
1–1985 Local Thermal Discomfort
4–1984 Methods for the Calculation of Contrast
Proper Use of Weighting Functions for Impact Testing
Computer Data Acquisition from Brüel & Kjær Digital Frequency Analyzers 2131/2134 Using their Memory as a Buffer

(Continued on cover page 3)

Technical Review

No. 1 · 1990

Contents

The Brüel & Kjær Photoacoustic Transducer System and its Physical Properties

by Jørgen Christensen, M.Sc.

Abstract

The Brüel and Kjær Multi-gas Monitor Type 1302 and the Toxic-gas Monitor Type 1306, both used for monitoring gases, are based on photoacoustic spectroscopy.

In photoacoustic spectroscopy (PAS) the gas to be measured is irradiated by intermittent light of pre-selected wavelength. The gas molecules absorb some of the light energy and convert it into an acoustic signal which is detected by a microphone. PAS is an inherently very stable method for detecting very small concentrations of gas.

In this article the Brüel & Kjær PAS transducer system is described, the acoustic signal generated by the gas is analyzed, and the influence of noise and other disturbing signals, which are likely to influence the performance of the system, are discussed.

Sommaire

Le Moniteur multigaz Type 1302 et le Moniteur de gaz toxiques Type 1306 Brüel & Kjær, destinés à la surveillance des gaz, utilisent le principe de la spectroscopie photoacoustique (SPA).

En SPA, le gaz à mesurer est irradié par une lumière intermittente de longueur d'onde prédéfinie. Les molécules de gaz absorbent une partie de l'énergie lumineuse qu'elles convertissent en un signal acoustique capté par un microphone. La méthode de mesure par SPA est très stable et permet de détecter de très faibles concentrations en gaz.

Les différents points traités dans cet article sont la description du système de transducteur photoacoustique Brüel & Kjær, l'étude du signal acoustique produit par le gaz et l'influence du bruit et des autres signaux parasites sur le fonctionnement du système.

Zussammenfassung

Der Multigasmonitor 1302 und der Gasmonitor 1306 von Brüel & Kjær sind Geräte zur Gasmessung, deren Meßprinzip auf der photoakustischen Spektroskopie (PAS) basiert.

Bei der photoakustischen Spektroskopie wird das zu messende Gas mit zerhacktem Licht einer gewählten Wellenlänge bestrahlt. Die Gasmoleküle absorbieren einen Teil der Lichtenergie und wandeln sie in ein akustisches Signal um, das mit einem Mikrofon gemessen werden kann. Die photoakustische Spektroskopie ist eine sehr stabile Methode, mit der sich sehr kleine Gaskonzentrationen erfassen lassen.

Der vorliegende Text beschreibt das PAS-Aufnehmersystem von Brüel & Kjær. Das durch das Gas erzeugte akustische Signal wird analysiert und der Einfluß von Hintergrundgeräuschen und anderen Störsignalen auf das Meßsystem werden diskutiert.

1. Introduction

The Brüel & Kjær Multi-gas Monitor Type 1302 and the Toxic Gas Monitor Type 1306, both used for monitoring toxic gases, are based on photoacoustic spectroscopy*.

In photoacoustic spectroscopy (PAS) some substance absorbs light energy and converts it to sound energy. PAS is an old science which was first investigated by Alexander Graham Bell in 1880. In Bell's experiment he placed the substance — in this case, cigar smoke — in a glass test tube. One end of a rubber tube was connected to the mouth of the test tube and the other end connected to the ear. By focusing intermittent sunlight onto the test tube, an audible sound was generated.

In the early 1970s interest in PAS was renewed because it offered a very sensitive method for the identification and quantification of trace amounts of atmospheric gas pollutants. Lasers were primarily used as the

---

* We have a patent for our photoacoustic gas monitors (at present only in the U.S.A. — Patent No. 4818882).

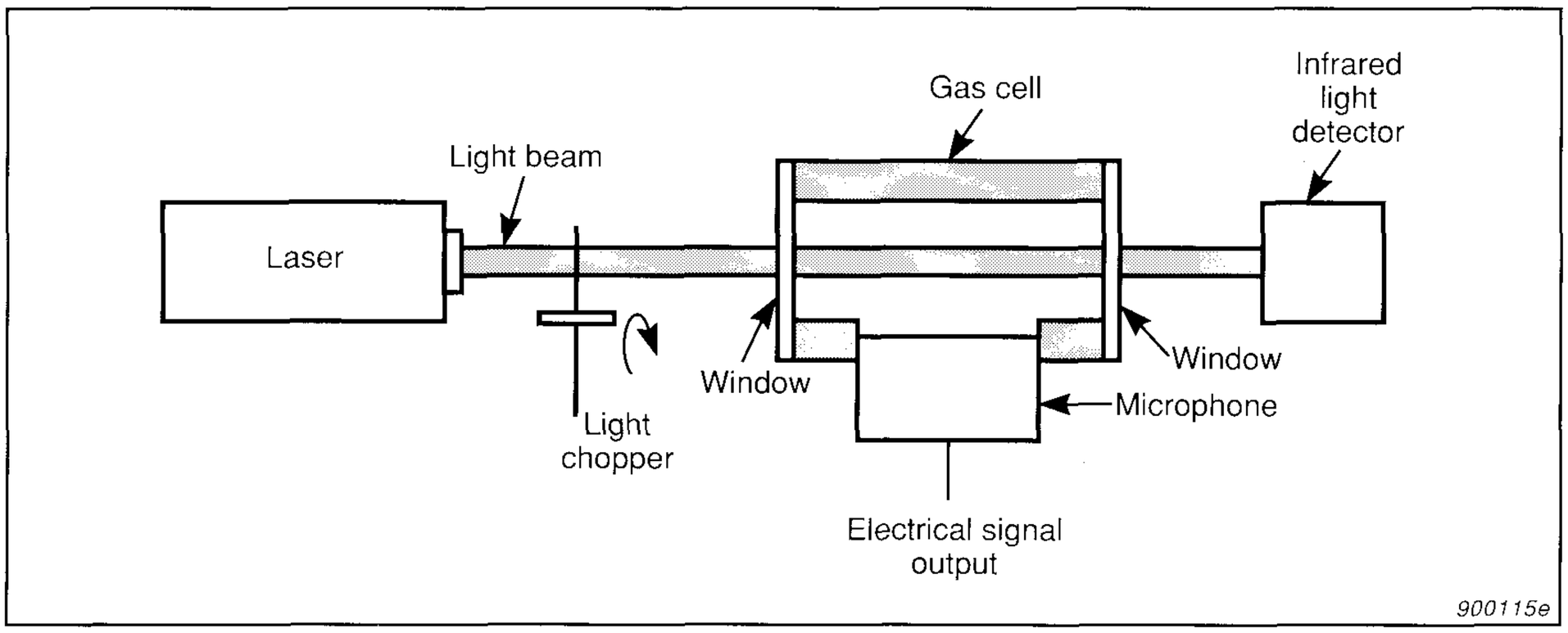

Fig. 1. Typical PAS system using a laser source

light (or excitation) source. The spectral region used was the infrared region as light in this region of the spectrum is capable of causing atoms in a molecule to vibrate. This is the physical mechanism responsible for the generation of the acoustic signal — translational energy transfer in the gas. The acoustic signal is detected, not by the ears as in the old days, but by a highly sensitive, low-noise microphone which converts the acoustic signal into an electrical signal for further processing. Fig. 1 shows the basic PAS set-up including a laser source; a rotating modulator or light chopper; a sealed gas cell with windows at both ends, to allow the laser light to pass through the cell; and a microphone to detect the acoustic signal. An IR (infrared) light detector is also shown — this measures the energy of the light after it has passed through the gas cell. The IR-detector is actually not part of a normal PAS-system, but it illustrates an alternative infrared spectroscopic method, namely the classical infrared transmission spectroscopic method used in many general purpose instruments and spectrophotometers.

If I_A is the amount of light energy absorbed by the gas, and I_T is the amount of light energy transmitted through the gas, then:

$$I_A + I_T = I_o \qquad (1)$$

where: I_o is the amount of light energy which would be transmitted through the cell if the gas in the cell absorbed no light energy.

In transmission spectroscopy, the absorbed energy I_A is found by measuring the amount of energy not absorbed in the cell, I_T, and subtracting this from I_o. At ppm (part per million) concentrations, I_A is typically 1000

times smaller than I_o and therefore this measurement requires an extremely stable measurement of the transmitted energy. However, in PAS the acoustic signal measured represents the amount of energy absorbed, and that is why the PAS measurement method offers far superior sensitivity and long term zero-point stability.

Among many other applications, microphones were being increasingly used by researchers in the field of photoacoustics around the world and this created the background for Brüel & Kjær's entry into the field of photoacoustics. Brüel & Kjær realized that mastering microphone technology was crucial to the development of a PAS-system with high sensitivity (minimum noise) and had already had many years of experience with the development and production of high quality microphones.

2. The Brüel & Kjær PAS Transducer System

In the initial stages of development of the Brüel & Kjær PAS system the goal was to produce a PAS transducer system which would form the "heart" of a small, lightweight and fully self-contained instrument suitable for the measurement of trace amounts of a wide variety of toxic gases, for example, those found in industry, hospitals and other areas.

One of the most important decisions to make was which kind of light source to use. The chosen source had to be compatible with the set goal —

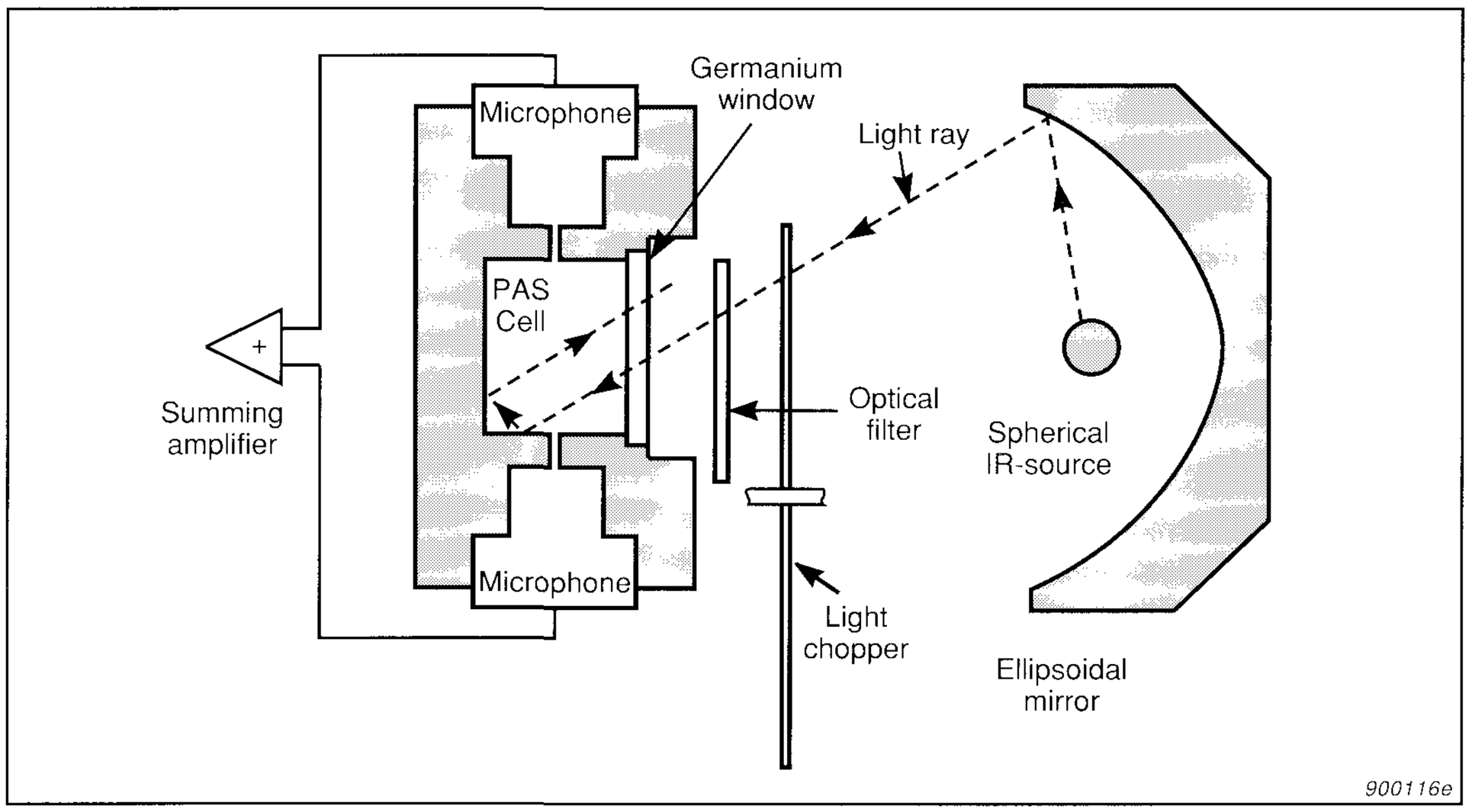

Fig. 2. Schematic cross-section of the Brüel & Kjær photoacoustic transducer system

it had to be an IR-source (infrared source) to fit with the absorption bands of most of the toxic gases; it had to be small, inexpensive and have a low power consumption. The choice fell on a black body source as it was a broad band source which largely covered the frequency range from 500 cm^{-1} to 4000 cm^{-1}, or in wavelength units, 20 μm to 2,5 μm. The selectivity necessary to make it possible to distinguish between gases, is obtained by appropriate filtering of the light. The carbon dioxide laser was a possible alternative light source which, in some cases, surpassed the "black body source" – "optical filter" combination with respect to sensitivity and selectivity. It had, however, one serious disadvantage, it had a limited frequency range. It covered, typically, 100 discrete frequencies in the range 900 – 1100 cm^{-1}, which limits the number of gases which could be measured. In addition, the carbon dioxide laser certainly did not fulfill the other requirements of small size, low cost and low power consumption.*

Fig. 2 shows the Brüel & Kjær PAS system. The IR-source is a spherical black body heated to approx. 800°C. Fig. 3 shows the spectral radiance L_ν of a black body source at different temperatures. As shown in Fig. 2 an ellipsoidal mirror focuses the light onto the window of the PAS cell after it has passed the light chopper and the optical filter. The chopper is a slotted disk which rotates and effectively "switches" the light on and off at a frequency of 20 Hz (the chopper frequency**). The optical filter is a narrow-band IR interference filter. Fig. 4 shows an example of an optical filter transmission curve. The Brüel & Kjær Toxic-gas Monitor Type 1306 has only one optical filter (as shown in Fig. 2). The Multi-gas Monitor Type 1302, however, may be equipped with 5–6 different optical filters mounted in a filter wheel.

---

* A few words about units may be appropriate. Light may be characterised by either its wavelength or its frequency — the latter usually measured in units of hertz (Hz). In spectroscopy, however, light frequency is most frequently given in units of "wave numbers" or "cm^{-1}", which represent the number of wavelengths that can be fitted into 1 centimeter. Thus, if you divide a wavelength measured in units of μm (10^{-6} m) into ten thousand (10^{+4}), you obtain the frequency in units of cm^{-1}. Alternatively, if you wish to convert frequency in Hz to a frequency in units of cm^{-1}, you just need to divide the frequency in Hz by the velocity of light (in units of cm/s). For example, a wavelength of 10 μm corresponds to a frequency of 1000cm^{-1} or $3 \cdot 10^{13}$ Hz.

** To avoid confusion, one should be aware that in PAS we use the term frequency in two different ways: we use it to describe the frequency of the light being used, and we use it to describe the chopper frequency which generates the pulsating light source. The chopper frequency is the same as the frequency of the photoacoustic signal generated when light is absorbed by the gas in the cell.

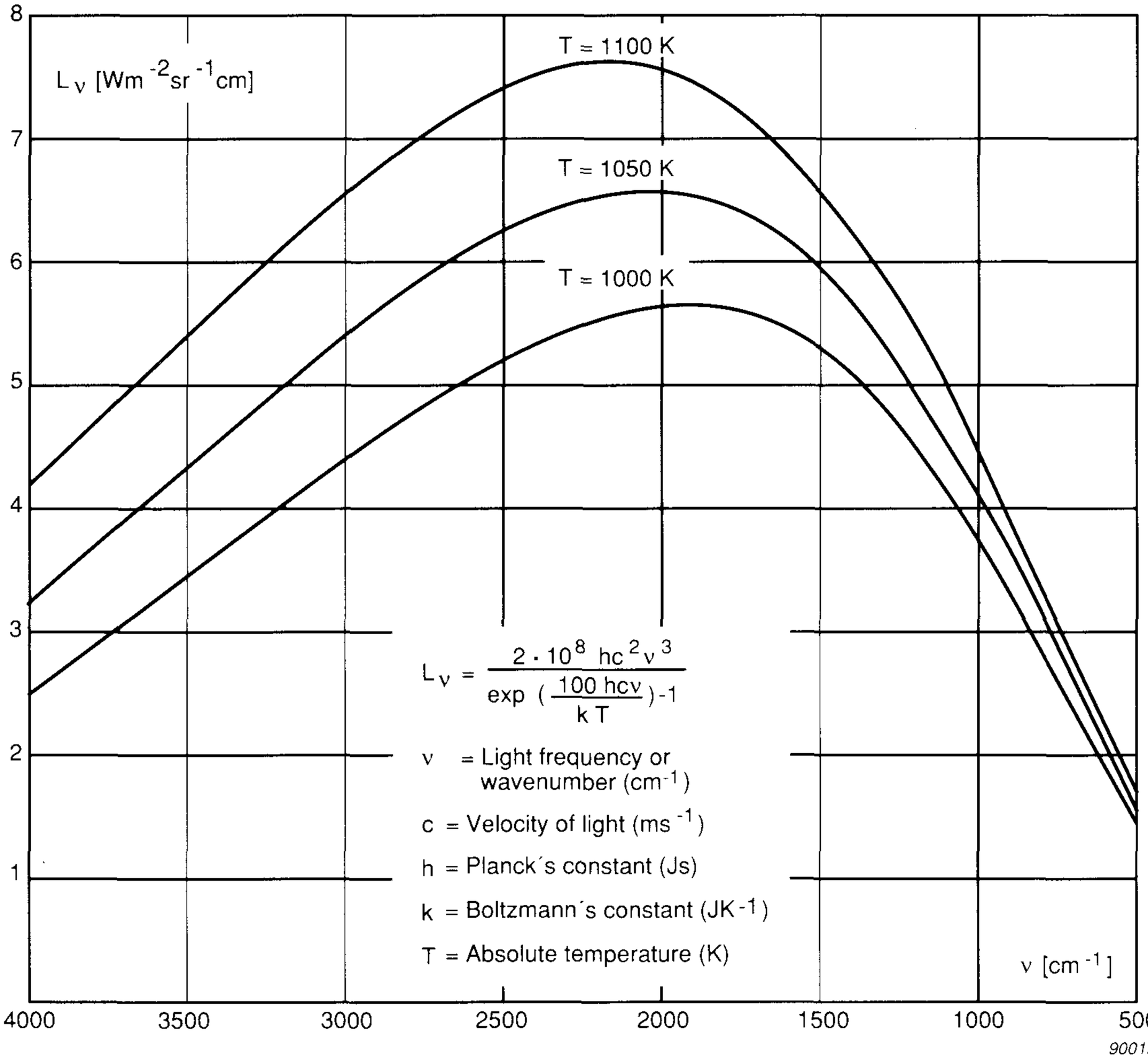

Fig. 3. Black-body spectral radiance L_ν

After passing through the germanium window, (see Fig. 2) the light beam enters the PAS-cell, which is an approx. 3 cm^3 cylindrical cavity. The surface of this cavity is polished and gold coated and therefore highly reflective. The light beam is reflected off the walls of the cell thus doubling its intensity. If the frequency of the light coincides with an absorption band of the gas in the cell, the gas molecule will absorb part of the light. The higher the concentration of gas in the cell, the more light will be absorbed. Fig. 5 illustrates the absorption spectrum of carbon monoxide. An appropriate optical filter for measuring *CO* will be the one shown in Fig. 4.

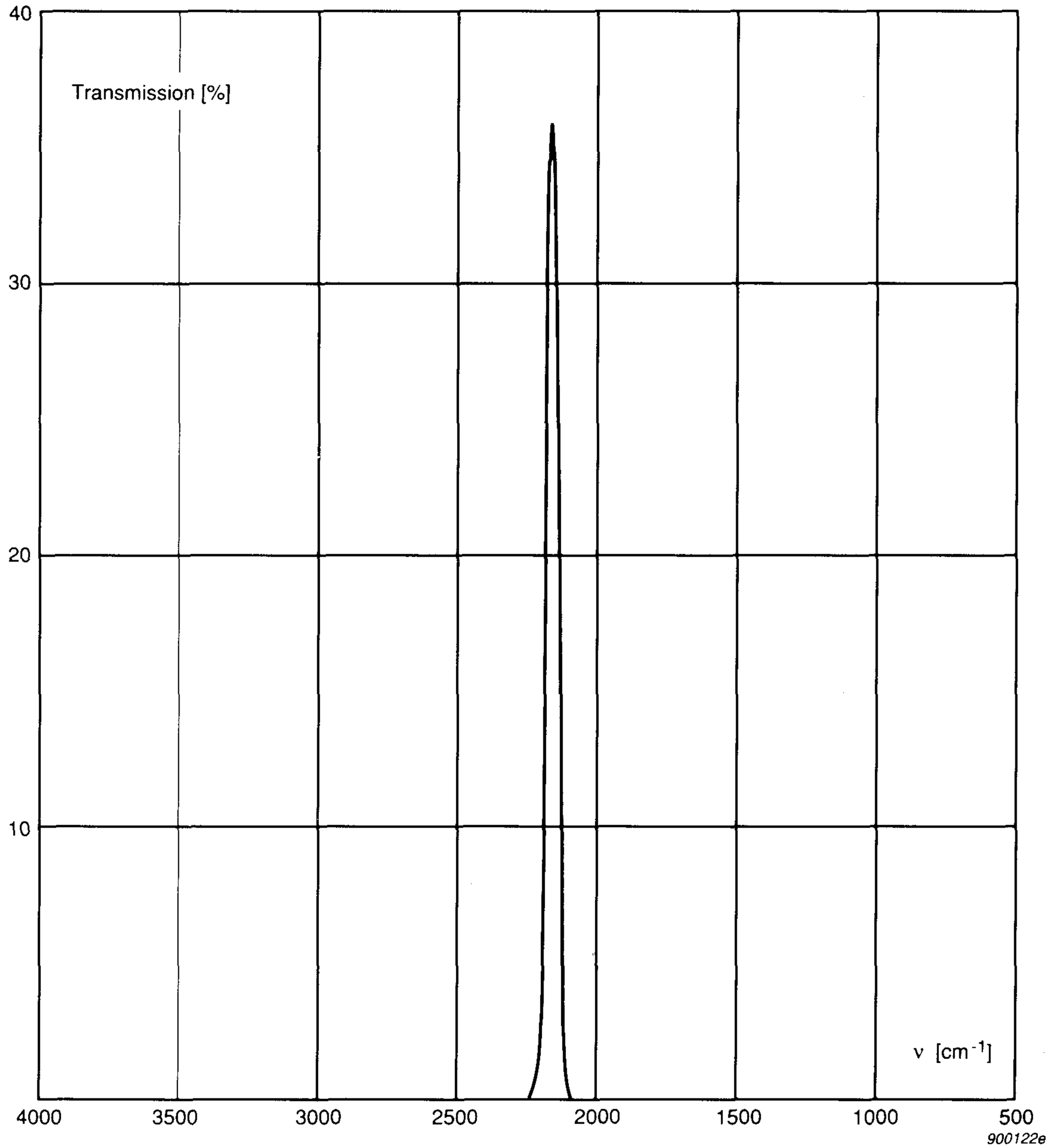

Fig. 4. Transmission characteristic of the optical filter no. UA 0984

Just a few words about absorption of light by molecules: the frequency of light in an absorption band corresponds to a vibrational resonant frequency of the atoms in the molecule. When this light is absorbed by the molecule it causes the atoms in the molecule to vibrate around their equilibrium positions. As the simplest possible example, let us consider a molecule

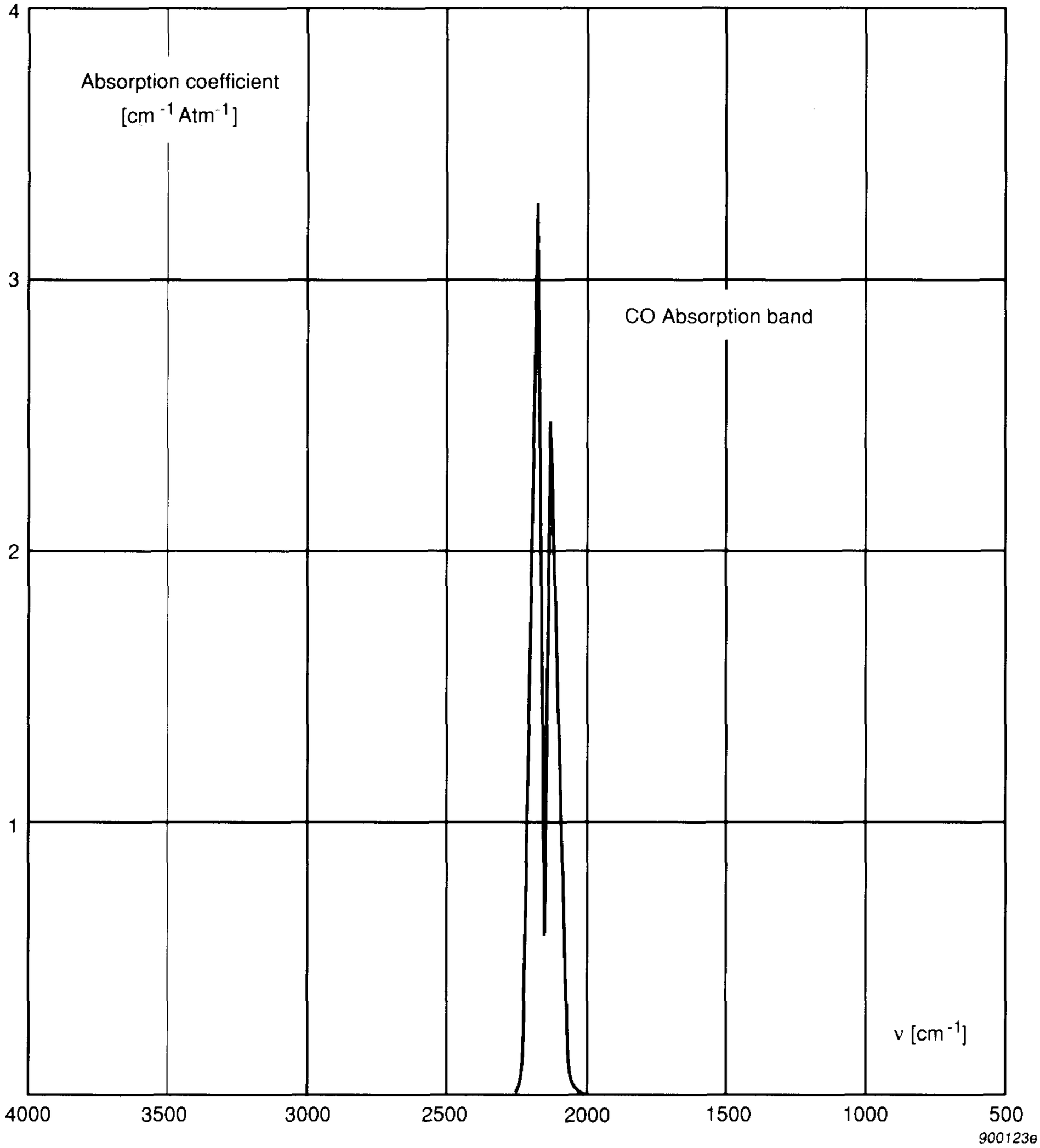

Fig. 5. Low resolution ($10\,cm^{-1}$) carbon monoxide (CO) absorption spectrum

consisting of only two different atoms A and B. Fig. 6 shows a simple, classical model of a diatomic molecule. The two atoms, with masses M_A and M_B respectively, are joined by a "bond", which maintains the atoms at some equilibrium separation, and has spring-like properties. The stiffness

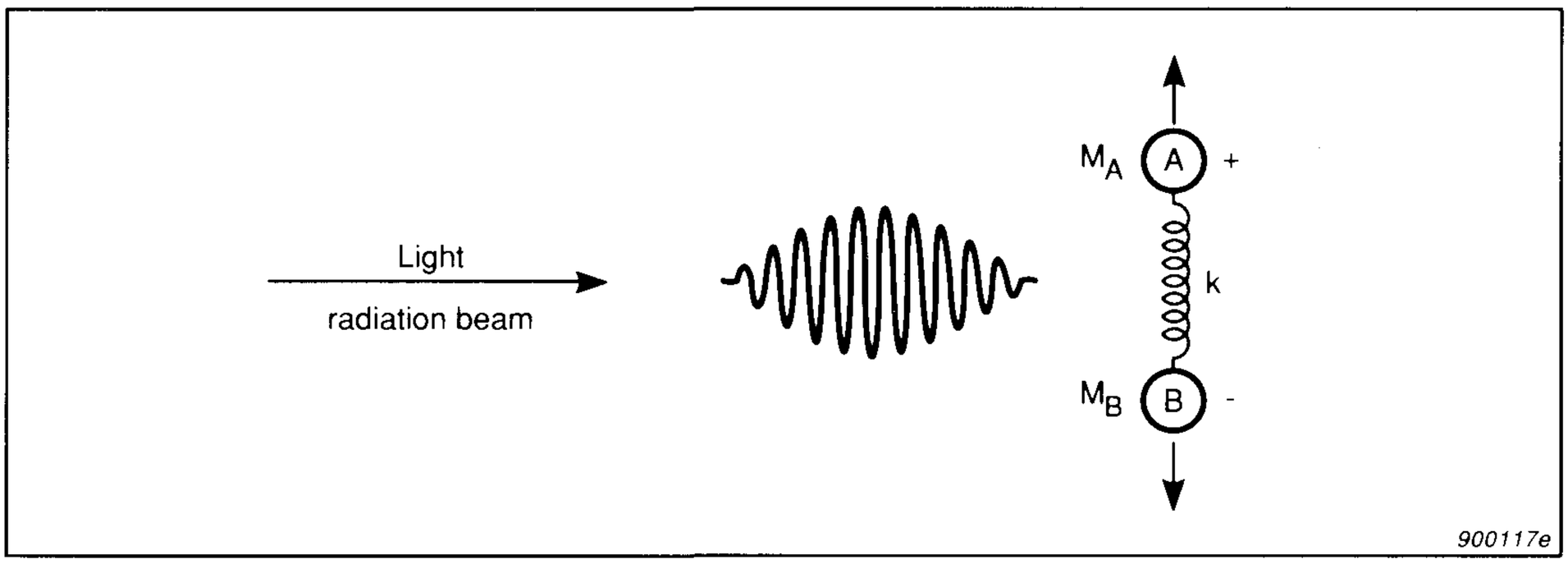

Fig. 6. Classical model for a diatomic oscillating molecule and its interaction with light

of the bond ("spring") can be characterized by a force constant k. According to this model, the diatomic molecule has only one resonant frequency:

$$\nu_o = \frac{1}{2\pi}\sqrt{\frac{k(M_A + M_B)}{M_A M_B}} \tag{2}$$

Most molecules possess an electrical dipole moment, e.g. CO does, while other molecules like O_2 and N_2 do not as they are absolutely symmetrical. Only 11 gases, in total, do not possess an electrical dipole moment (the nobel gases *He*, *Ne*, *Ar*, *Kr*, *Xe* and *Rn* and the gases H_2, N_2, O_2, F_2, and Cl_2). If the frequency of the incident light corresponds to the resonant frequency ν_o of the molecule, then the light, which is electromagnetic radiation, will interact with the electrical dipole of the molecule and cause the atoms in the molecule to vibrate. These vibrations are damped by collisions with other molecules which are present causing vibrational energy to be very quickly converted to molecular translational energy, in other words, heat. The heated gas expands and causes a pressure rise, and as the light is chopped, the pressure will alternately increase and decrease — an acoustic signal is thus generated. If the intensity of the incident light is I_o, we get a sound pressure (p):

$$p = \frac{K(\gamma - 1)\, c\, I_o}{f} \tag{3}$$

where $\gamma = C_p/C_v$, C_p and C_v is the heat capacity of the gas mixture in the cell at constant pressure and constant volume respectively, c is the gas concentration, f is the chopper frequency and K is a constant depending on the selected filter and gas. The acoustic signal is detected by the two microphones which are acoustically connected to the cell via narrow channels, and the electrical output signals from the two microphones are added in a summation amplifier, before they are electronically processed.

The PAS system also includes an air pump for drawing an air sample into the PAS cell, and two magnetic valves, which are only open when a new sample of air is drawn into the cell.

A light detector, mounted in the mirror assembly, monitors the light from the infrared source. The detector signal is used to stabilise the temperature of the infrared source.

The temperature of the bulk of the PAS cell is likewise monitored. This enables the photoacoustic signal to be compensated for its dependence on temperature.

In the following sections, we will analyze in detail how the photoacoustic signal is generated and study the various noise- and disturbing signals. However, before we do that we will take a quick look at molecular spectroscopy.

3. A primer on molecular spectroscopy

In the previous section we used a classical model of a diatomic molecule (AB) and found that it had only one resonance frequency. This is clearly not in agreement with what we see in the absorption spectrum of CO shown in Fig. 5 which shows two resonances close to each other. If one looks at the high resolution absorption spectrum of CO illustrated in Fig. 7 we can see that these two resonances, or absorption bands, are each split into a large number of very narrow lines. The classical theory is obviously wrong, or at least, not complete. We have to turn to quantum theory to provide an adequate description of molecular spectroscopy.

In quantum theory electromagnetic radiation can be regarded as a stream of particles — photons — each with the energy $h\nu$, where h is Planck's constant, and ν is the classical frequency (that is, the frequency of the incident light). Quantum theory expresses the vibrational energy of a molecule in terms of a series of discrete energy levels E_0, E_1, E_2 etc. (see Fig. 8). Each molecule must therefore have a vibrational energy which is equivalent to one of these energy levels. In a large assembly of molecules

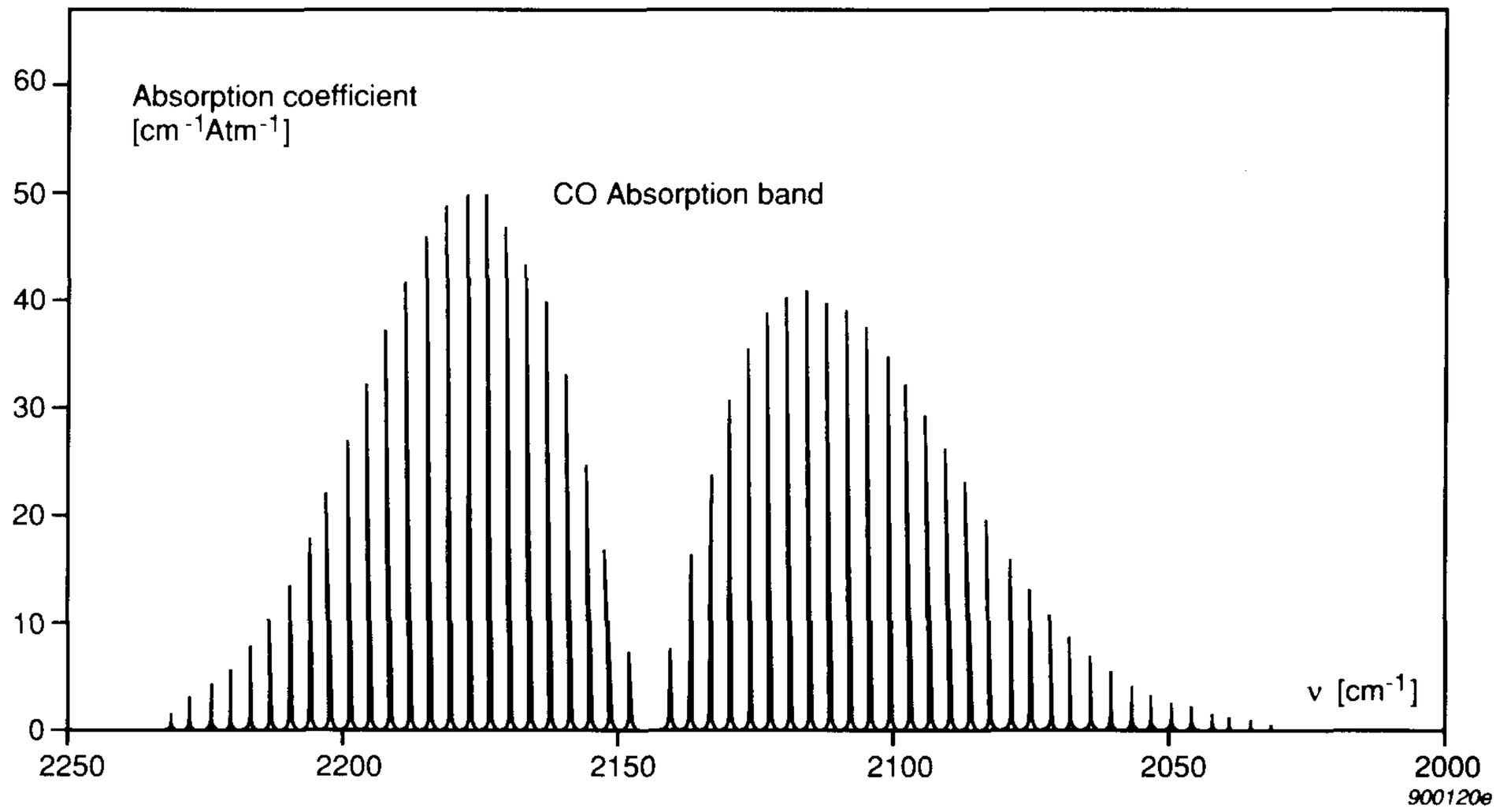

Fig. 7. High resolution (0,01 cm^{-1}) CO absorption spectrum in expanded view

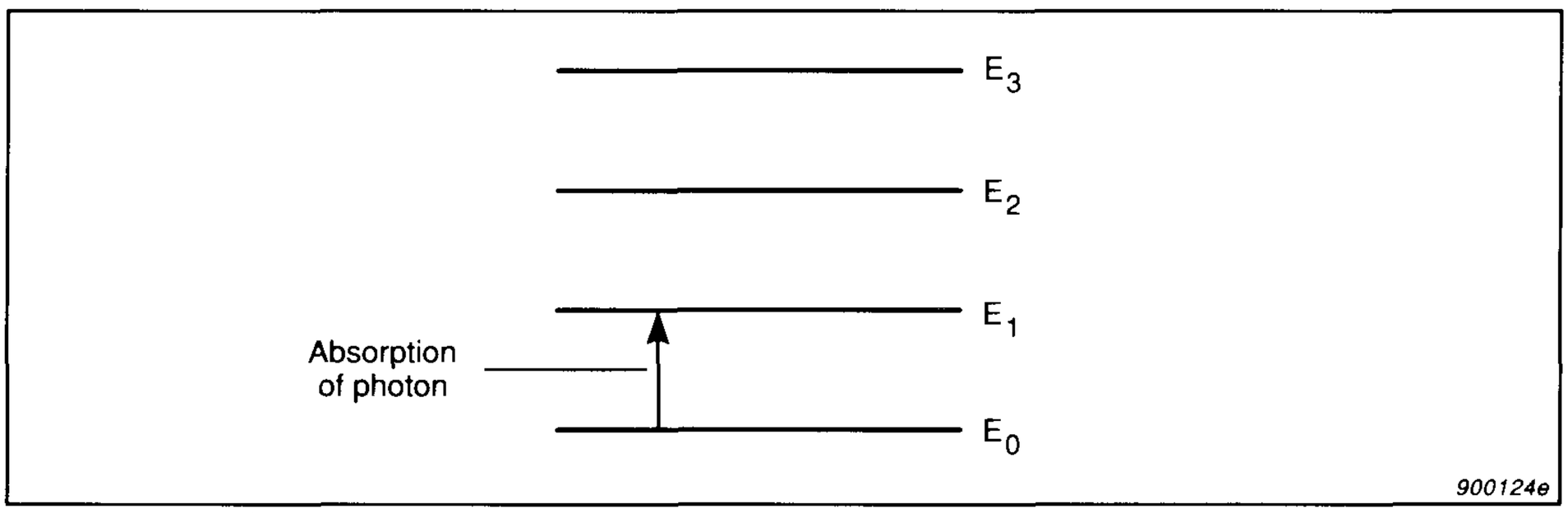

Fig. 8. Molecular vibrational energy levels

there will be a distribution of all the molecules between these various energy levels. The relative population of molecules N_i / N_j, in any two levels E_i and E_j, when in thermal equilibrium, is given by the Maxwell-Boltzmann equation which for our purposes can be expressed as:

$$\frac{N_i}{N_j} = e^{-\frac{E_i - E_j}{kT}}, \tag{4}$$

where k is the Boltzmann Constant and T is the absolute temperature.

The necessary condition for light to cause a molecule to vibrate, or — using the terminology from quantum theory — to excite the molecule from energy state E_i to energy state E_j, is that the photon energy $h\nu$ be equal to the energy difference $E_j - E_i$. Hence, the frequency of light required to cause a transition from energy level E_0, which represents the non-vibrating ground-state, to energy level E_1 is given by:

$$\nu = \frac{(E_1 - E_0)}{h} \tag{5}$$

For a CO molecule, the frequency corresponding to the E_0 to E_1 transition, is 2143 cm^{-1}. When in thermal equilibrium at 20°C, we find, using (4) and (5) that $N_i / N_0 \approx 3 \cdot 10^{-5}$ which implies that practically all the CO molecules are in their non-vibrating ground state, that is having an energy E_o.

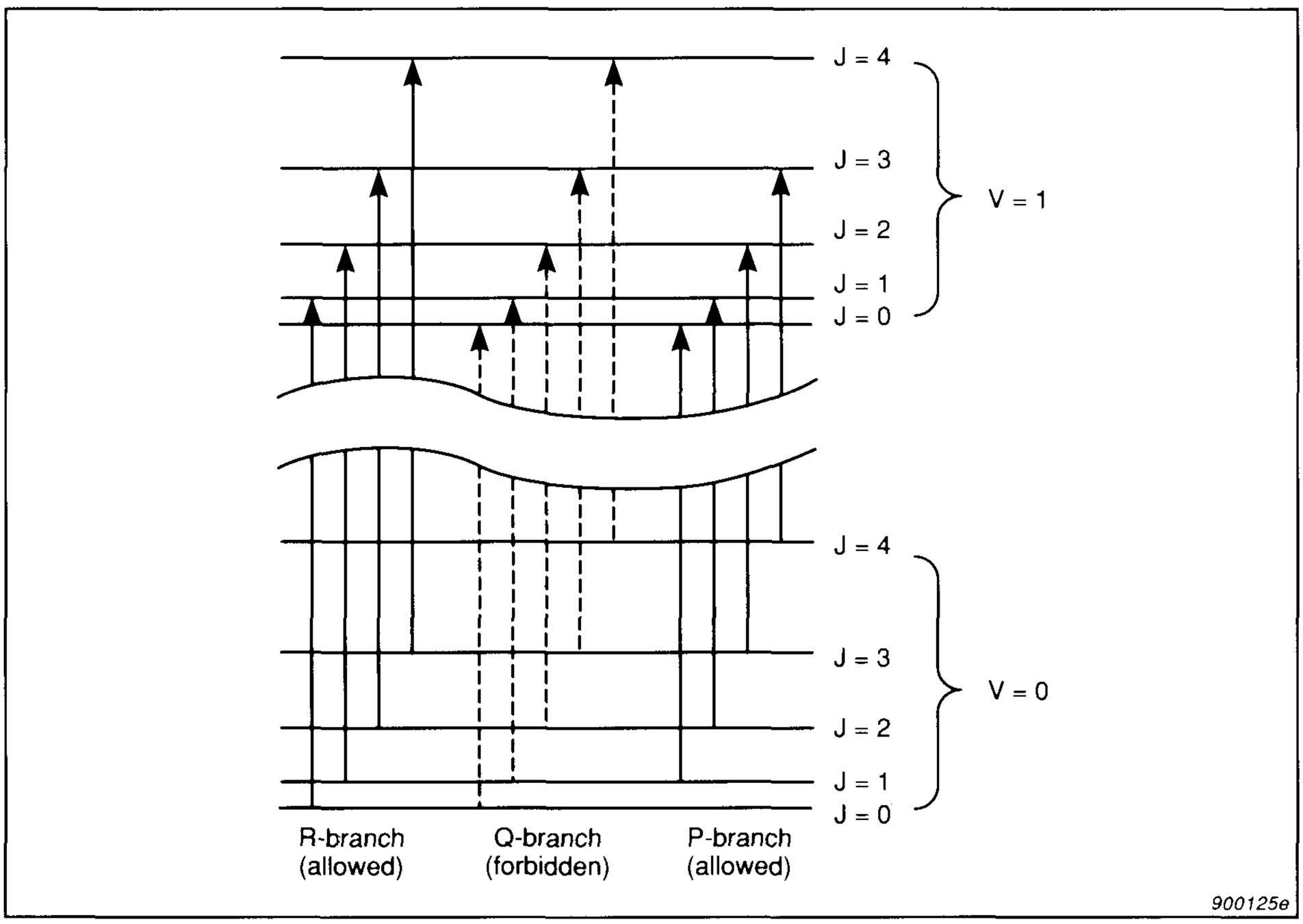

Fig. 9. Energy levels and associated vibration-rotation transitions for a diatomic molecule

Molecules not only vibrate, they also rotate, and in quantum theory the rotational energies are likewise expressed as a series of discrete energy levels, but with much smaller differences between the energy levels than for the vibrational energy levels. Each of the vibrational energy levels are thus split into a series of levels. This is shown in Fig. 9 for the two lowest vibrational energy levels ($V = 0$ and $V = 1$), and the five lowest rotational energy levels ($J = 0$ to $J = 4$). The fine structure of the CO band is due to simultaneous changes in vibrational and rotational energy levels. Not all transitions are possible. For a diatomic molecule such as CO, the transitions corresponding to the first four bands on each side on the centre of the band, are shown in Fig. 9. It is noticed, that a vibrational transition with no change in rotational energy (the $Q-$branch) is not possible. This explains why the CO molecule does not absorb light at the fundamental vibration frequency of 2143 cm^{-1}, which is the calculated expected centre frequency for the absorption band using classical theories of physics.

4. The Photoacoustic Gas Signal

In this section we shall describe how the photoacoustic signal is generated, and evaluate the performance of the PAS system under the constraint of a black-body source.

a. The light input into the PAS cell

When a perfectly reflecting mirror is used to focus light from a black-body source, it can be shown that the spectral intensity of the light at the focus point is:

$$I_\nu = \pi L_\nu \sin^2 \theta \tag{6}$$

where I_ν is the spectral intensity (intensity per unit frequency), L_ν is the spectral radiance of a black body according to Planck's law of radiation (Fig. 3) and θ is the half cone angle of the light cone. Using the laws of thermodynamics, the I_ν value obtained using a perfectly reflecting ellipsoidal mirror can be shown to be equal to the theoretical upper limit using a black body source of spectral radiance L_ν. When $\theta = \pi/2$, I_ν reaches its maximum value of πL_ν.

Another way of increasing spectral intensity (I_ν) is by increasing L_ν. This is done by increasing the temperature of the black body source. In practice, however, there are certain limits as to how high its temperature should be allowed to go.

In a laser PAS system (as in Fig. 1) the θ value is very low and this allows the laser beam to pass through the cell without hitting the cell walls. This is advantageous because when light hits the walls some of it is absorbed and converted into heat energy which generates an unwanted signal. If the design of the laser PAS system was adapted for use with a black body source, the light intensity would be very small, due to the $\sin^2\theta$ term, so this was obviously not the solution. We chose to solve the problem by: (1) using divergent light (with the highest possible θ value) to obtain maximum light intensity; (2) making the surface of the inner walls of the cell highly reflective and heat absorbing to minimise the unwanted signal; and finally (3) measuring the small unwanted "wall" signal so that the total measured signal in the cell (gas signal + "wall" signal) could be compensated for the "wall"-signal contribution, thus leaving the signal produced by the gas in the cell.

To ensure that the highest possible light energy enters the PAS cell, the intensity of light over the whole surface of the PAS cell window (aperture), which is placed in the focus plane, should equal the intensity at the source's focus point. The intensity distribution in the focus plane depends on the source/mirror configuration. Fig. 10 illustrates three different source/mirror configurations and shows the computer-calculated corresponding relative light intensity along the diameter of each aperture. In all three cases, the same θ value and source diameter were used. The best choice is the upper one.

A θ value equal to $\pi/2$, for highest possible light intensity, is in practice not possible because the centre frequency of an optical interference filter depends, to some extent, on the angle of incidence of the light. This limits θ to about 30°. There are other factors which limit the light intensity, for example: the source's emissivity is limited because it is not an ideal black body; some of the light reflected from the surface of the mirror and the PAS cell is lost; and some of the light transmitted by the optical filter and the cell window is lost. The intensity of the light entering the PAS cell can be expressed as:

$$\alpha\, T_f\, \pi\, L_\nu \sin^2\theta\ \ \Delta\nu \tag{7}$$

where $\Delta\nu$ is the bandwidth of the light, T_f is the optical filter transmission and α is a factor representing all other losses.

This formula describes the non-intermittent light intensity, but we are more interested in the intensity of the intermittent light. This corre-

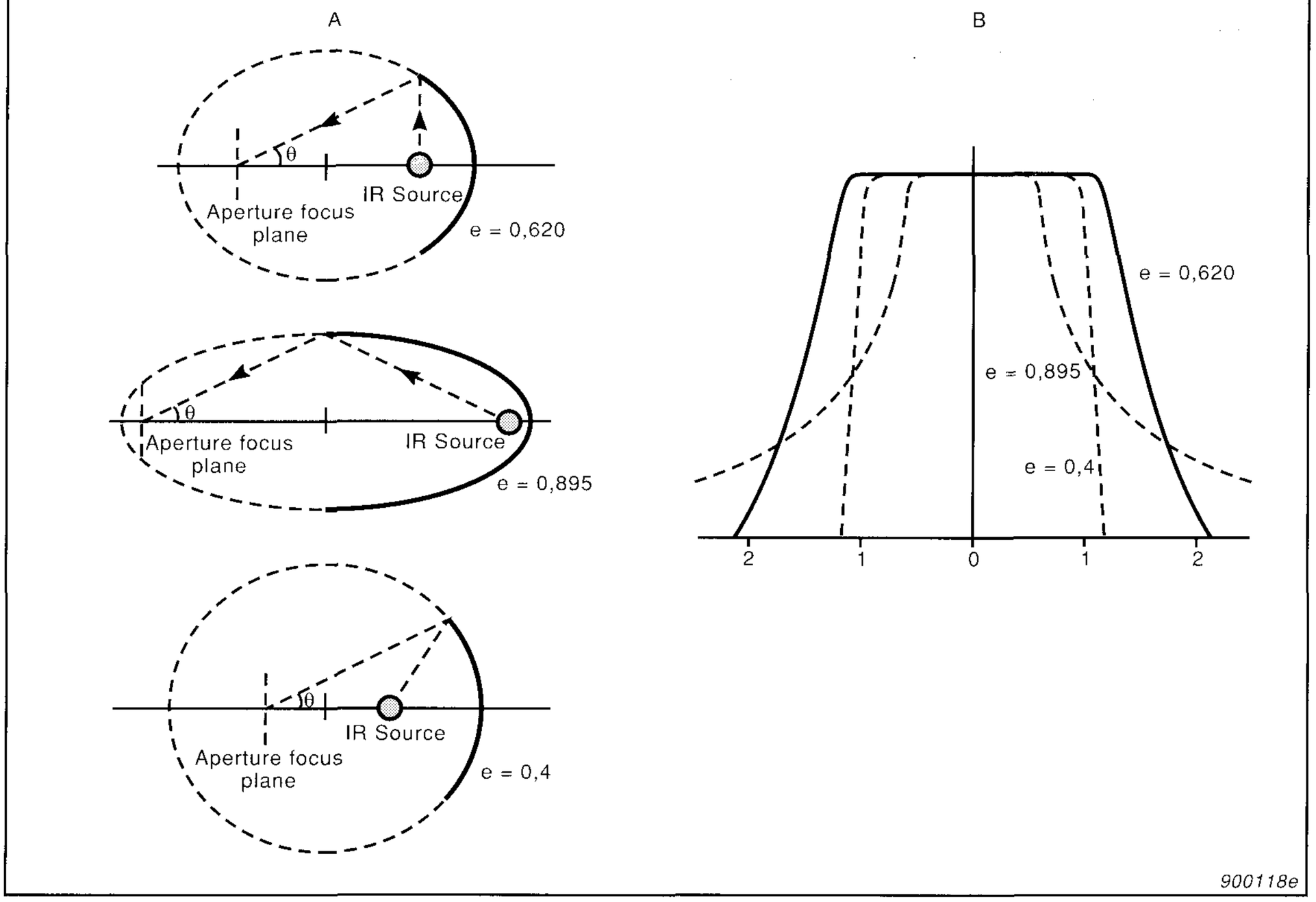

Fig. 10. A: Three different mirror/source configurations characterised by the excentricity of their corresponding ellipsoids. The half-cone angle, θ, and the diameter of the spherical IR-source are the same in all three cases.
B: The relative light intensity along the diameter of the aperture focus plane, in units of the IR-source diameter for each mirror/source configuration

sponds to the sinusoidal component of the light intensity at the chopper frequency. Assuming square chopped light, then:

$$I(t) = I_o \ \mathrm{e}^{j\omega t}, \tag{8}$$

and: $$I_o = 2\alpha \ T_f \ L_\nu \sin^2\theta \ \ \Delta\nu, \tag{9}$$

where I_o is obtained by multiplying the non-intermittent light intensity (7) by $2/\pi$.

b. Absorbed light power

The transmission of light through an absorbing gas is described by Beer's law:

$$I(l) = I(o)\, e^{-ckl} \ , \tag{10}$$

where c is the gas concentration, k is the absorption coefficient of the gas and l is the length of the light path. Hence, gas absorbs some of the light and its intensity is reduced by:

$$I(o) - I(l) = I(o)\left(1 - \mathrm{e}^{-ckl}\right) \approx ckl\, I(o) \ , \tag{11}$$

the latter approximation being valid for low absorption.

The absorbed power per unit volume in the PAS cell, $W(t)$, is found by dividing the absorbed intensity by the length of the cell, noting that the length of the light path due to the end reflection is approximately twice the cell length, and by replacing $I(o)$ by the light intensity $I(t)$ entering the PAS cell:

$$W(t) = 2\, ck\, I(t) \ = W_o\, e^{j\omega t} \ , \tag{12}$$

where, by using (8) and (9) we find:

$$W_o = 2\, ck\, I_o = 4\, \alpha\, T_f\, L_\nu \sin^2\theta\, ck\, \Delta\nu \tag{13}$$

c. Generation of the acoustic signal

Next we will consider the acoustic signal generated by the absorbed light power. This is determined by the differential equation:

$$\kappa\, \nabla^2 T = \rho_o\, C_p\, \frac{\partial T}{\partial t} - \frac{\partial p}{\partial t} - W(t) \ , \tag{14}$$

where: κ , ρ_o , C_p: thermal conductivity, mass density and heat capacity of the gas mixture in the cell

T : the gas temperature signal

p : the acoustical pressure signal

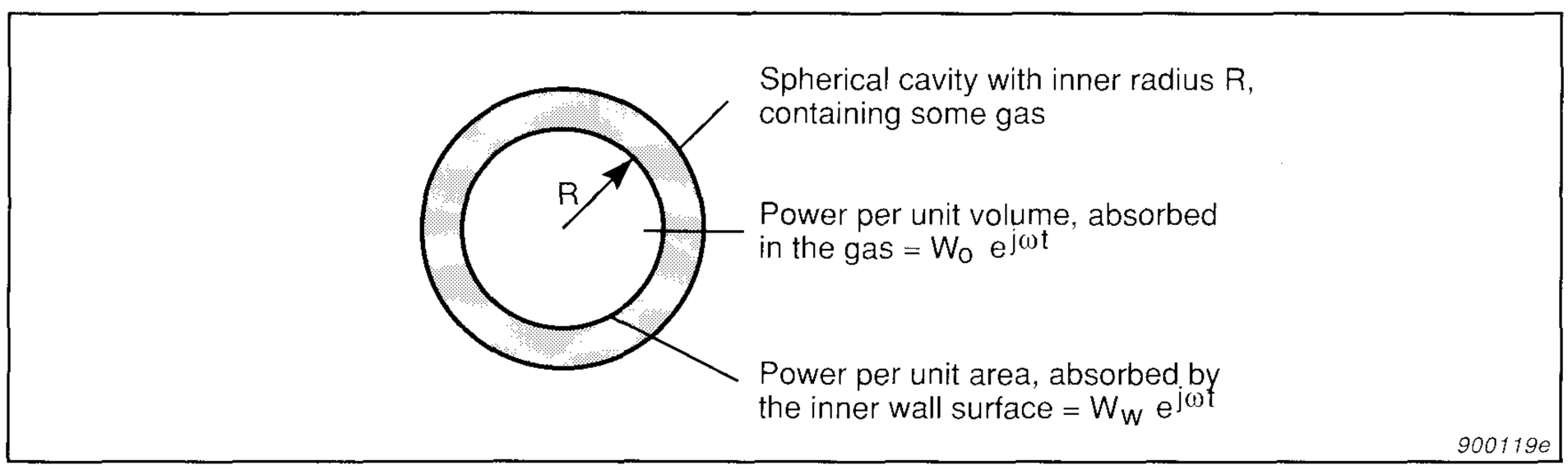

Fig. 11. A spherical cavity used as a model for calculating the acoustic signal due to the absorption of energy by either the gas in the cavity or by the inner wall surface.

In order to solve this equation, we will use the simplest possible geometry, that is a spherical cavity with inner radius R (see Fig. 11). Furthermore, we will consider the steady state solution only, corresponding to the sinusoidal varying absorbed power $W(t) = W_o\, e^{j\omega t}$.

Hence $T(t) = \tau_o(r)\, e^{j\omega t}$ and $p(t) = p_o\ e^{j\omega t}$ are substituted into the differential equation assuming spherical coordinates described by r :

$$\frac{\partial^2 \tau_o(r)}{\partial r^2} + \frac{2}{r}\,\frac{\partial \tau_o(r)}{\partial r} - \lambda^2 \tau_o(r) = -\frac{j\omega p_o + W_o}{\kappa} \tag{15}$$

where: $$\lambda^2 = \frac{j\omega\ \rho_o C_p}{\kappa} \tag{16}$$

We are assuming W_o to be independent of r, which is approximately the case in the PAS cell. Likewise we assume p_o to be independent of r. This is also a very good approximation because at 20 Hz, the wavelength of sound (17 m) is much larger than the diameter of the cavity (2 cm).

The boundary condition is that $\tau_o(R)$ be equal to zero, which supposes that the wall material has a much higher heat capacity than that of the gas. When we solve the equation, we first find $\tau_o(r)$; then, by integration over the volume of the cavity, we find its average value; and finally, by using the gas equation of state to eliminate τ_o, we find the amplitude of the acoustic signal:

$$p_o = \frac{W_o(\gamma - 1)}{\omega}\ e^{-j\frac{\pi}{2}}\ S \tag{17}$$

$$\text{where } S = \frac{1 - \frac{3}{\lambda R}\left[\coth(\lambda R) - \frac{1}{\lambda R}\right]}{1 + \frac{3(\gamma - 1)}{\lambda R}\left[\coth(\lambda R) - \frac{1}{\lambda R}\right]} \tag{18}$$

The factor $e^{-j\frac{\pi}{2}}$ represents a phase lag of $\pi/2$.
The RMS value of the pressure signal becomes:

$$p_{\text{RMS}} = \frac{\sqrt{2}}{2} \frac{W_o(\gamma - 1)}{\omega} \left| S \right| \tag{19}$$

The parameter S describes the low frequency behaviour. If a thermal diffusion length in the gas mixture is much smaller than R, then S will be close to one. A thermal diffusion length μ is equal to:

$$\mu = \sqrt{\frac{2\kappa}{\omega \rho_o C_p}} \tag{20}$$

At 20 Hz, μ = 0,56 mm in atmospheric air. With R = 0,9 cm, corresponding to a volume of the cavity of 3 cm^3, then $\mu << R$. By calculating $|S|$ from the formula, we find $|S| \approx 0{,}9$.

The transfer function of the cell, p_o / W_o is a complex quantity representing both magnitude and phase, the input signal being the absorbed power per unit volume. Fig. 12 shows the magnitude, that is, of $|p_o| / W_o$, on a logarithmic scale as function of the chopper frequency $f = \omega/2\pi$ (Curve a). At higher frequencies, $|p_o| / W_o$ is inversely proportional to the chopper frequency as indicated by the high frequency asymptote (Curve d). At low frequencies $|p_o| / W_o$ tends towards a constant value as indicated by the low frequency asymptote (e). At a frequency f = 0,48 Hz, $|p_o| / W_o$ is equal to $\sqrt{2}/2$ times its low frequency value. If an analogy is made with electrical network theory, the thermal time constant of the PAS cell is found to be $\tau = 1/\omega$ = 0,33 s.

The curves a and b show the influence of cell size, Curve b shows the magnitude of $|p_o| / W_o$ for a cell with R = 3 cm. In the high frequency range, $|p_o| / W_o$ is independent of cell size, but in the low frequency range $|p_o| / W_o$ becomes greater by the ratio of the radii squared, and the thermal time constant is increased by the same amount.

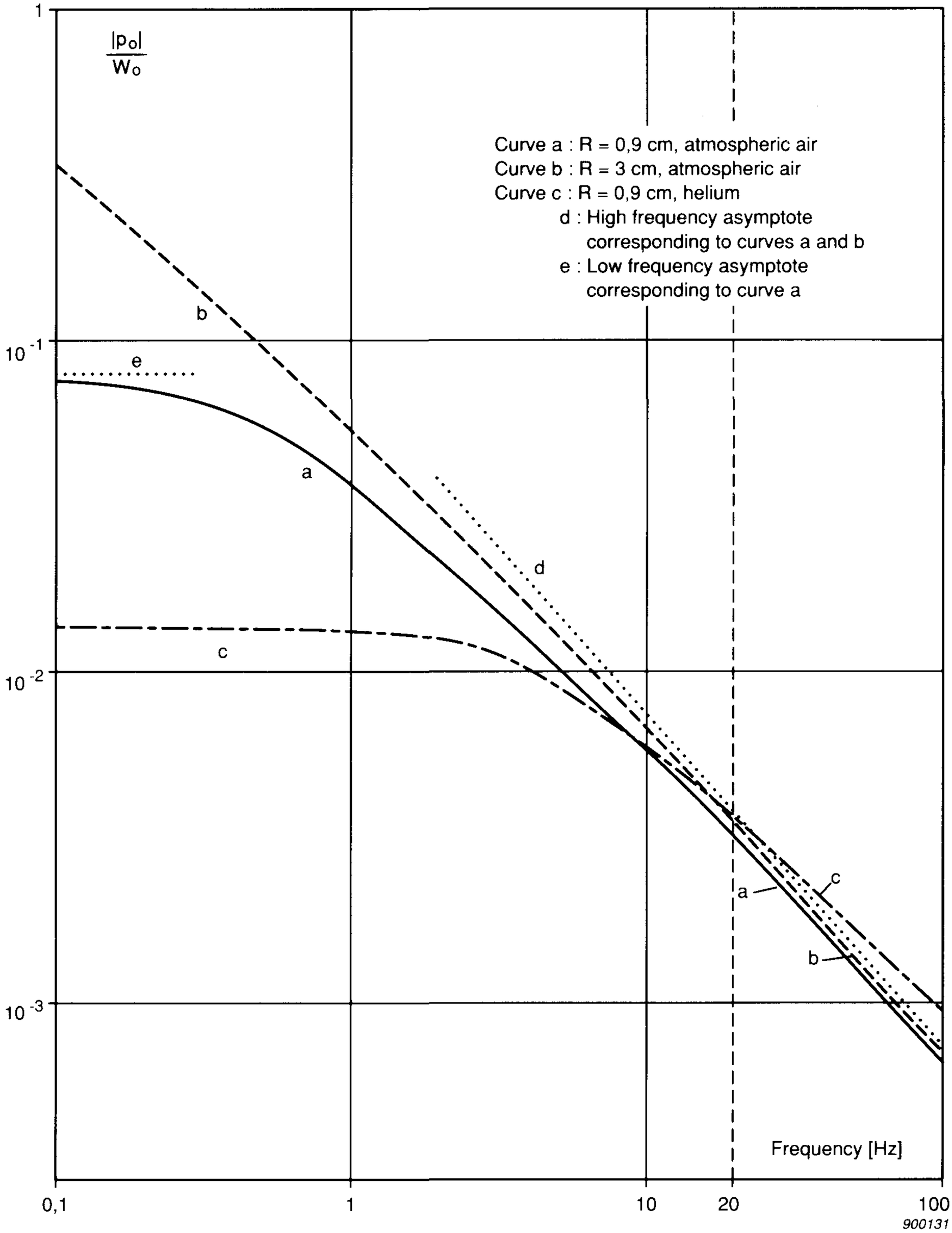

Fig. 12. The transfer function $|p_o| / W_o$ of a spherical cavity (see Fig. 11)

$|p_o| / W_o$ is related to the physical parameters γ, κ, ρ_o and C_p of the gas and this is significant if the gas mixture in the cell is not atmospheric air. This is illustrated in Fig. 12 by curve *c* and curve *a*. Curve c assumes helium to be the basic gas in the cell, curve a assumes atmospheric air to be the basic gas in the cell. The cell size for both curves is the same. Because helium has a higher $(\gamma - 1)$ value = 0,63, the signal at higher frequencies is greater than that with atmospheric air. However, due to the high thermal conductivity of helium, the low frequency cut off occurs at a much higher frequency, thus resulting in a lower level in the low frequency range.

The corresponding phase curves are not shown. The phase lag is 90° in the high frequency range and 0° in the low frequency range. The phase lag on curve a at 20 Hz is equal to 83°.

d. The Detection Limit

The value of the acoustic signal generated (p_o) is independent of the shape of the cell in the high frequency range because it corresponds to the purely adiabatic condition. (We are only considering non-resonant conditions). At lower frequencies the shape of the cell does, however, play a role. The Brüel & Kjær PAS cell has cylindrical geometry while the solution (17) is valid for a cell with spherical geometry. If, however, the volumes of the cylindrical and the spherical cells are equal, and the cylindrical cell's diameter to length ratio is close to 1, the spherical solution gives a sufficiently good overall approximation.

We will have to add one more correction. In the actual PAS-system, there is certain "dead" space, due to air channels, microphone volumes, etc. which shunt the acoustic signal. This dead space is corrected for by multiplying by a factor of 0,85. By using $|S| = 0{,}9$, we find for our cylindrical PAS cell:

$$p_{\mathrm{RMS}} = \frac{\sqrt{2}}{2} \cdot 0{,}85 \cdot 0{,}9 \frac{(\gamma - 1)}{\omega} W_o = 0{,}54 \frac{(\gamma - 1)}{\omega} W_o \qquad (21)$$

and, by inserting W_o (13),

$$p_{\mathrm{RMS}} = \frac{2{,}16 (\gamma - 1) \alpha T_f L_\nu \sin^2\theta \, c k \Delta\nu}{\omega} \qquad (22)$$

With the Brüel & Kjær PAS system $\theta = 33°$, $\omega = 2\pi\,(20\ \mathrm{Hz})$ and $\gamma - 1 =$ 0,4 as for atmospheric air. Further, α has been found to be equal to 0,55. Hence,

$$p_{\mathrm{RMS}} = 1{,}13 \cdot 10^{-3}\ T_f\ L_\nu\ c\ k\ \Delta\nu, \qquad \text{or:}$$

$$1{,}13 \cdot 10^{-3}\ T_f \int F(\nu - \nu_o)\ L_\nu\ k(\nu)\, d\nu \tag{23}$$

where the final expression is a more stringent formulation which takes into account the transmission function of the optical filter, $F(\nu - \nu_o)$.

The detection limit of a gas is defined as the gas concentration causing a signal equal to twice the RMS noise level of the transducer. As we shall see later, the RMS noise level in the Brüel & Kjær PAS system is equal to $2{,}5 \cdot 10^{-6}$ Pa. Hence, the detection limit can be written as:

$$\begin{aligned}\text{Detection limit} &= \frac{4{,}4 \cdot 10^{-3}\ [\,\mathrm{Wm^{-3}\,sr^{-1}}\,]}{T_f \int F(\nu - \nu_o)\ \ L_\nu k(\nu)\, d\nu} \\ &\approx \frac{4{,}4 \cdot 10^{-3}\ [\mathrm{Wm^{-3}\,sr^{-1}}]}{T_f\ L_\nu\ k\,\Delta\nu}\end{aligned} \tag{24}$$

As an example, let us consider the measurement of CO using the optical filter UA 0984 (Fig. 4). By computer calculation, using the CO absorption spectrum as shown in Fig. 7,

$$\int F(\nu - \nu_o)\, L_\nu\, k(\nu)\, d\nu = 8{,}25 \cdot 10^4 \quad [\mathrm{Wm^{-2}\,sr^{-1}\,m^{-1}\,Atm^{-1}}] \tag{25}$$

With $T_f = 0{,}37$, the CO detection limit is calculated to be $1{,}5 \cdot 10^{-7}$ Atm or 0,15 Vol. ppm. The calculated CO signal, using 54 ppm CO, becomes $1{,}86 \cdot 10^{-3}$ Pa. To compare the theoretical and practical detection limits, a measurement of the signal produced by a CO concentration of 54 ppm was performed — it was found to be $1{,}97 \cdot 10^{-3}$ Pa, which is in quite close agreement with the calculated signal. This, however, is no coincidence, as the loss factor α, was found by comparing the calculated and measured gas signals using CO as well as many other different gases and optical filters.

Finally, a few figures may be worth mentioning. The RMS value of the gas temperature signal at the detection limit is equal to $2 \cdot 10^{-8}$ °C. The RMS deflection of the microphone membrane at the detection limit is equal to $3 \cdot 10^{-14}$ m, which is approximately ten times the radius of the electron or the approximate size of a proton.

e. The effect of molecular relaxation

In section 4 c, it was implicitly assumed that all of the absorbed light energy was immediately converted to heat. This is usually the case if the conversion is fast enough so that it does not interfere with the generation of the acoustic signal at a chopper frequency of 20 Hz. There are, however, some exceptions.

When a gas molecule absorbs a photon and goes from its ground energy state E_o to an excited state E_1 no heat is generated. The molecule can then lose its absorbed energy by returning to its ground energy state in one of the following ways:

1. It can re-radiate (emit) a photon.
2. It can collide with another molecule of the same species which is in its ground energy state E_0, and excite it to the excited state E_1.
3. It can collide with a molecule of a different species and excite it from its ground state to some excited state.
4. It can collide with and transfer its energy to another molecule in the gas and thereby increase the translational energy of the molecule it collides with.

It is the fourth process which produces the photo-acoustic signal, as increased translational energy is simply increased heat energy. If the rate of this process is much faster than the rate at which the light is chopped, then the assumption of immediate conversion of absorbed energy to heat is a valid approximation. All four processes compete with each other but, in general, the fourth process is by far the fastest, hence all of the absorbed energy is converted into heat energy.

If, however, the fourth process is not the dominating process, or if the rate of the fourth process is too slow, then it will affect both the magnitude and phase of the generated acoustic signal. In order to correctly calculate the signal, the differential equation would have to be modified and it would be much more difficult to solve. Let us consider a particular measurement to illustrate the point:

Suppose we want to perform a span calibration for measuring CO, using a calibration gas mixture of say 50 ppm CO in dry nitrogen. Because of its

lack of an electric dipole moment, a N_2 molecule cannot be brought to a vibrationaly excited state by interaction with light. However, if an excited CO molecule collides with a N_2 molecule, which is the collision process most likely to occur, then the N_2 molecule can be excited while at the same time the CO molecule is "de-excited" (it goes back to its ground energy state). The vibration frequency of a N_2 molecule is approximately 2330 cm^{-1}, and is close enough to that of a CO molecule (2143 cm^{-1}) to make this vibrational energy exchange a very likely process at normal temperatures. The rate of the process, which corresponds to the third process in the list, is fast, and this makes it the dominating one. Once the N_2 molecule has captured the CO molecule's vibration energy, it is very reluctant to give it up as translational energy as the nitrogen molecule is known to take an extremely long time to "relax". This results in the generation of only a very small photo-acoustic signal. Because the vibrational frequency of N_2 is greater than that of CO, the gas mixture actually cools down when it absorbs energy because the vibrational energy exchange requires a small contribution of translational energy. This phenomenon is sometimes referred to as kinetic cooling.

This problem is solved by adding some water vapour to the calibration gas. Water molecules prove to be very efficient catalyzers in the relaxation process. In practice water vapour is easily added to the gas mixture by passing the dry calibration gas mixture through a "vapour tube", which is strongly permeable to water vapour but not permeable to CO. The gas passing through the "vapour tube" is thus humidified to the same humidity level as that of the ambient air.

Carbon dioxide (CO_2) and nitrous oxide gas (N_2O) behave in much the same way as carbon monoxide (CO), if they are measured by a filter which transmits light whose wavelength coincides with their strongest absorption band, as they can so easily transfer their energy to nitrogen molecules. In general, however, this problem is rare.

5. The noise signals

As we discussed in Section 4a, the use of a black body source imposes certain limitations on the level of the photoacoustic signal. However, as sensitivity is ultimately determined by the signal to noise ratio, an alternative method of increasing sensitivity is to reduce the noise and other

disturbing signals as much as possible. There are several contributors to the total noise signal. Contributions can be roughly categorised as:

- ○ The wall signal
- ○ The window signal
- ○ Acoustic noise
- ○ Vibration noise
- ○ The dust signal
- ○ Microphone/preamplifier noise

a. The Wall Signal

The wall signal is due to the absorption of light by the surface of the cell walls, this causes a periodic increase in the temperature of the cell wall at the chopper frequency. The increase in the temperature of the wall surface causes heat to flow by conduction to the air layer in contact with the walls, causing it to expand. As the light is periodic the air in contact with the wall will expand and contract at the frequency of the chopper and thus generate an acoustic signal. The wall signal has been calculated for the case with the spherical cavity (Fig. 11) by solving a proper differential equation, in much the same way as the gas signal was calculated. We will not treat the solution in detail as the complete expression of the wall signal is considerably more complicated than the gas signal expression. However, it is worth noting that the high frequency approximation of the acoustic signal amplitude is a good approximation at 20 Hz:

$$p_w = \frac{3\gamma P_o W_w}{\omega R T_o \left[\rho_w C_w \kappa_w \frac{\rho_o C_p}{\kappa} \right]^{1/2}} \cdot e^{-j\frac{\pi}{2}} \tag{26}$$

where W_w : absorbed power per unit wall surface area
ρ_w, C_w, κ_w : mass density, heat capacity and thermal conductivity of the wall material
ρ_o, C_p, κ : mass density, heat capacity and thermal conductivity of the gas mixture in the cell
P_o, T_o : ambient pressure and temperature respectively
R : cell radius
ω : chopper frequency
γ : C_p/C_v of the gas mixture in the cell

The conditions necessary for this approximation to be correct are: that a thermal diffusion length in the gas as well as in the wall is small compared to R; and further, that the wall is sufficiently thicker than the thermal diffusion length in the wall. At low frequencies, these conditions are not fulfilled and therefore a simple formula cannot be used. However, the low frequency behaviour of the wall signal with regard to its amplitude and phase, is largely similar to that of the gas signal. Hence, the gas signal to wall signal ratio is largely independent of frequency.

W_w is proportional to the light intensity hitting the cell walls and to the absorptivity of the wall surface. Thus, in order to minimize the wall signal:

- ○ The absorptivity of the wall surface must be low or its reflectivity be high
- ○ The cell radius should be large
- ○ The product $\rho_w C_w \kappa_w$ should be high

The wall signal also depends on the gas mixture in the cell as the parameters γ, ρ_o, C_p and κ are gas dependent. For example, if helium is the only gas in the cell, the wall signal is found to be approximately 3 times greater than when atmospheric air is in the cell.

The typical size of a measured wall signal is $1{,}5 \cdot 10^{-4}$ Pa, which corresponds to a total power of 1 mW_{RMS} of light power being absorbed by the cell walls.

The wall signal is typically 20 times the detection limit signal. It is, however, a well defined and stable signal whose temperature dependence has been mapped with each of the optical filters which are available for installation in the 1302 or 1306. When a zero-point calibration is performed using a certain optical filter, a zero gas, e.g. clean, dry synthetic air, is drawn into the cell and the signal in the cell is measured — this is the wall signal. After a zero-point calibration the instrument will be able to automatically compensate for the wall signal and therefore the gas signal can be calculated. Because the temperature of the PAS cell is monitored the wall signal can be compensated for its temperature dependence and therefore the compensation for the wall-signal contribution can be performed at various ambient temperatures.

b. The Window Signal

A small fraction of the light incident on the window will be absorbed by the window material and this will cause a temperature fluctuation on the window surface. Just as the absorption of light by the cell walls generates an

acoustic signal the absorption of light by the window material also generates an acoustic signal — a "window signal".

If the low frequency behaviour of the window signal and its phase are not taken into account, the window signal amplitude can be expressed by the following equation:

$$p_{wi} = \frac{2\sqrt{2}\ \gamma P_o \beta I_o}{l_c T_o \omega^{3/2} \left[\frac{\rho_o C_p}{\kappa}\right]^{1/2} C_{wi}\ \rho_{wi}} \tag{27}$$

Where: β : absorption coefficient of window material
C_{wi} : heat capacity of window material
ρ_{wi} : mass density of window material
l_c : internal length of cylindrical PAS cell

The window signal differs from the wall signal in the following respects: (1) the frequency dependence of the window signal is inversely proportional to $\omega^{3/2}$ instead of ω; and (2) the window signal is independent of the thermal conductivity of the window material. Both these differences are due to the fact that light is absorbed by the whole bulk of the window material whereas it is only absorbed by the surface of the cell wall.

Using germanium as the window material, β is highly dependent on the purity of the material, the worst case value is stated as 2 m^{-1}. To illustrate, take the example of the optical filter UA 0984 (Fig. 4), $I_o = 47\ W/m^2$ (see equation (9)). Using the β value given above, the RMS value of the window signal is found to be $9{,}5 \cdot 10^{-6}$ Pa. This signal is typically found to be 15 times smaller than the wall signal. However, as the signal measured during a zero-point calibration (using a non-absorbing gas) includes both the wall signal and the window signal, a zero-point calibration automatically takes into account both signal contributions.

c. Acoustic Noise

If acoustic noise from the environment is transmitted to the microphones in the PAS cell, it has the potential to disturb the measurement. The PAS cell, being a closed volume, will attenuate the noise, the amount of attenuation depending on the mechanical stiffness and the air-tightness of the cell.

As a model for estimating the attenuation, let us consider a cylindrical volume, with a and b being the inner and outer radius respectively, and with inner length l_c.

At first, let us suppose that the cylindrical ends are closed by plates with infinite stiffness. The attenuation factor can be expressed as:

$$\frac{E\left[\,1-\left(\,\frac{a}{b}\right)^2\,\right]}{(5-2\,\sigma)\,\gamma\;P_o}\;, \tag{28}$$

Where: E : Young's modulus or longitudinal elasticity
σ : Poisson's ratio
γ : C_p/C_v for the gas mixture in the cell
P_o : Ambient pressure

Now, let us suppose that a window with finite stiffness is placed on the one end only, as the endplate on the other end in the PAS cell is much more stiff than the window, due to its thickness. We assume that the window is mounted with a fixed edge, which is approximately the case. The attenuation factor is now expressed by:

$$\frac{1}{\left[\,\frac{5-2\,\sigma}{\left[\,1-\left(\frac{a}{b}\right)^{\,2}\,\right]E}+\frac{a^4\left(1-{\sigma_o}^2\right)}{16\,E_o\,t^3\;l_c}\right]\gamma\;P_o}\;, \tag{29}$$

Where: E_o : Young's modulus for the window material
σ_o : Poisson's ratio for the window material
t : thickness of the window

Take a numerical example: a = 7,6 mm, b = 12 mm, $E = 1{,}3 \cdot 10^{11}$ Pa and σ = 0,34 (copper). In the first case with 2 stiff end-plates the attenuation is found to be equal to $1{,}3 \cdot 10^5$. Even if b was infinitely large, the attenuation would be equal to $2 \cdot 10^5$, which is only a slight improvement.

In the second case, with a window at one end, the window material being germanium with $E_o = 9{,}4 \cdot 10^{10}\ P_a$ and σ_o = 0,3, the window thickness t = 1,5 mm and the cell length l_c = 17,5 mm, the attenuation is found to be $8 \cdot 10^4$, i.e. the attentuation is only slightly reduced.

One could fear, that the magnetic valves, although closed, could potentially be a path for transmitting sound, but measurements of the attenuation at 20 Hz shows typical values of $1 \cdot 10^5$, which is in close agreement with the calculated values in spite of the simplicity of the model.

It is necessary to discuss one more point. The microphone, being a condenser microphone, includes a back volume with a small vent to ensure static pressure equalisation. If this vent is led out to the ambient air, it will create a path for transmitting external sound backwards to the microphone membrane. To avoid this problem a dedicated PAS microphone was developed, for use in the Brüel & Kjær PAS system. In the PAS microphone the vent is connected to the PAS cell volume instead of the ambient air, as is the case with standard Brüel & Kjær microphones.

Fig. 13 shows a typical low-frequency acoustic noise spectrum as measured in an office environment using a Brüel & Kjær FFT analyzer. The

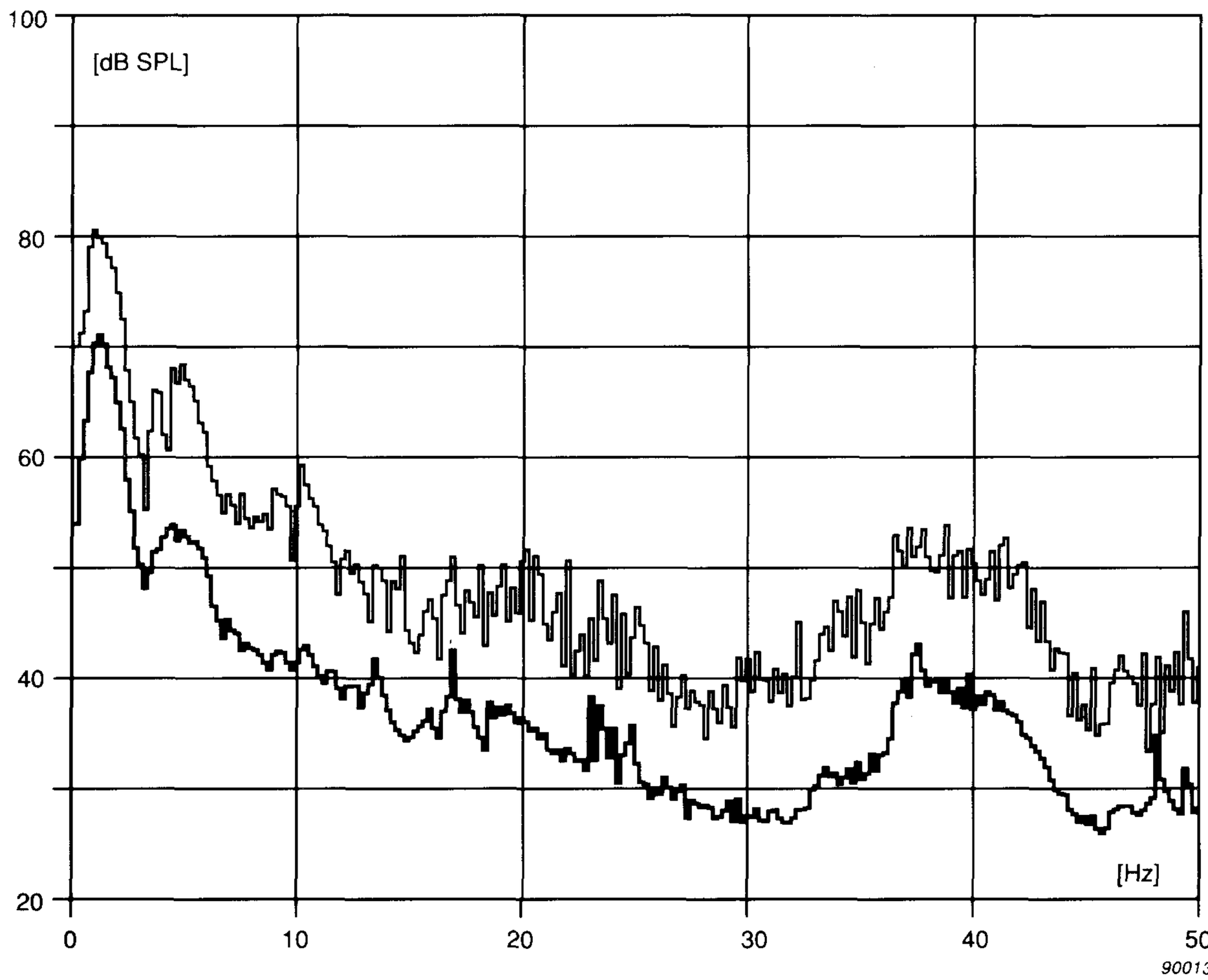

Fig. 13. Low frequency acoustic RMS noise spectrum in an office environment. Upper curve: maximum, lower curve: average

bandwidth is 1/8 Hz, which is largely equal to the bandwidth used in 1302/1306. The upper curve shows the maximum level, and the lower curve the average level. Reading from the upper curve, at 20 Hz the max. level is equal to 50 dB SPL, or $6{,}3 \cdot 10^{-3}$ Pa, causing a sound pressure of $6{,}3 \cdot 10^{-8}$ Pa inside the cell. This is a factor of 80 below the detection limit. In this particular case acoustic noise from the environment will therefore not be a problem. In general, acoustic noise from the environment is not a problem.

d. Vibration noise

Vibration of the PAS cell, caused by vibrations always present in the environment, can be a potential source of noise and give rise to a microphone signal.

A noise signal is created by the vibration of the mass of the microphone membrane and the mass of air in the cell as well as by deformation of the PAS cell.

At low frequencies, the microphone membrane can be likened to a piston. When it is exposed to a vibration, only the vibration component perpendicular to the membrane will affect it. An acceleration $a_o \sin \omega t$ will be equivalent to a pressure $p_m = \rho_m d\, a_o \sin \omega t$ where ρ_m is the mass density of the membrane material and d is the thickness of the membrane. With $\rho_m = 8{,}9 \cdot 10^3\ \mathrm{kg/m^3}$ and $d = 2\,\mu\mathrm{m}$, $p_m = 1{,}8 \cdot 10^{-2}$ Pa at an acceleration of 1 $\mathrm{ms^{-2}}$ RMS.

The next point to consider is the confined air mass in a closed cell. When this mass is exposed to vibration, the pressure in a plane through the centre of gravity of the air mass, and perpendicular to the direction of vibration, will remain unchanged. At a distance x from the plane, the pressure signal will be equal to $p_{\mathrm{air}} = \rho_o x\, a_o \sin \omega t$, where ρ_o is the mass density of the gas mixture in the cell. With $\rho_o = 1{,}2\ \mathrm{kg/m^3}$ (atm. air) and $x = 15$ mm, $p_{\mathrm{air}} = 1{,}8 \cdot 10^{-2}$ Pa at an acceleration of 1 $\mathrm{ms^{-2}}$ RMS, i.e. the same pressure as that due to the microphone membrane.

In the Brüel & Kjær PAS system, vibration sensitivity has been significantly reduced by using a differential set up with two microphones. The two identical microphones are symmetrically placed around the centre of symmetry of the PAS cell, and in addition they are mounted face to face. The signal output from each microphone is added together and thus the gas signal is doubled. Any linear acceleration produced by vibration of the membrane mass as well as the air mass, cancel each other out when the two microphone signals are added.

Care has been taken to make the amplitude and phase of the microphones identical. The vibration amplitude sensitivity of a microphone depends upon parameters such as membrane stiffness and membrane mass. The phase of a microphone depends on its low frequency cut off, which is determined by the equalization vent. The low frequency vibration response of a condenser microphone is equal to the acoustic frequency response obtained when the vent is outside the sound field. This is advantageous because the phase deviation at 20 Hz is then less sensitive to variations in the low-frequency cut-off when compared to the usual acoustic frequency response where the vent is in connection with the sound field. Any small differences in amplitude and phase which still remain are compensated for electronically.

The need for low vibration sensitivity also made it necessary to thoroughly consider the preamplifier design and its connection to the microphone so that the balancing-out of the vibration signals was not compro-

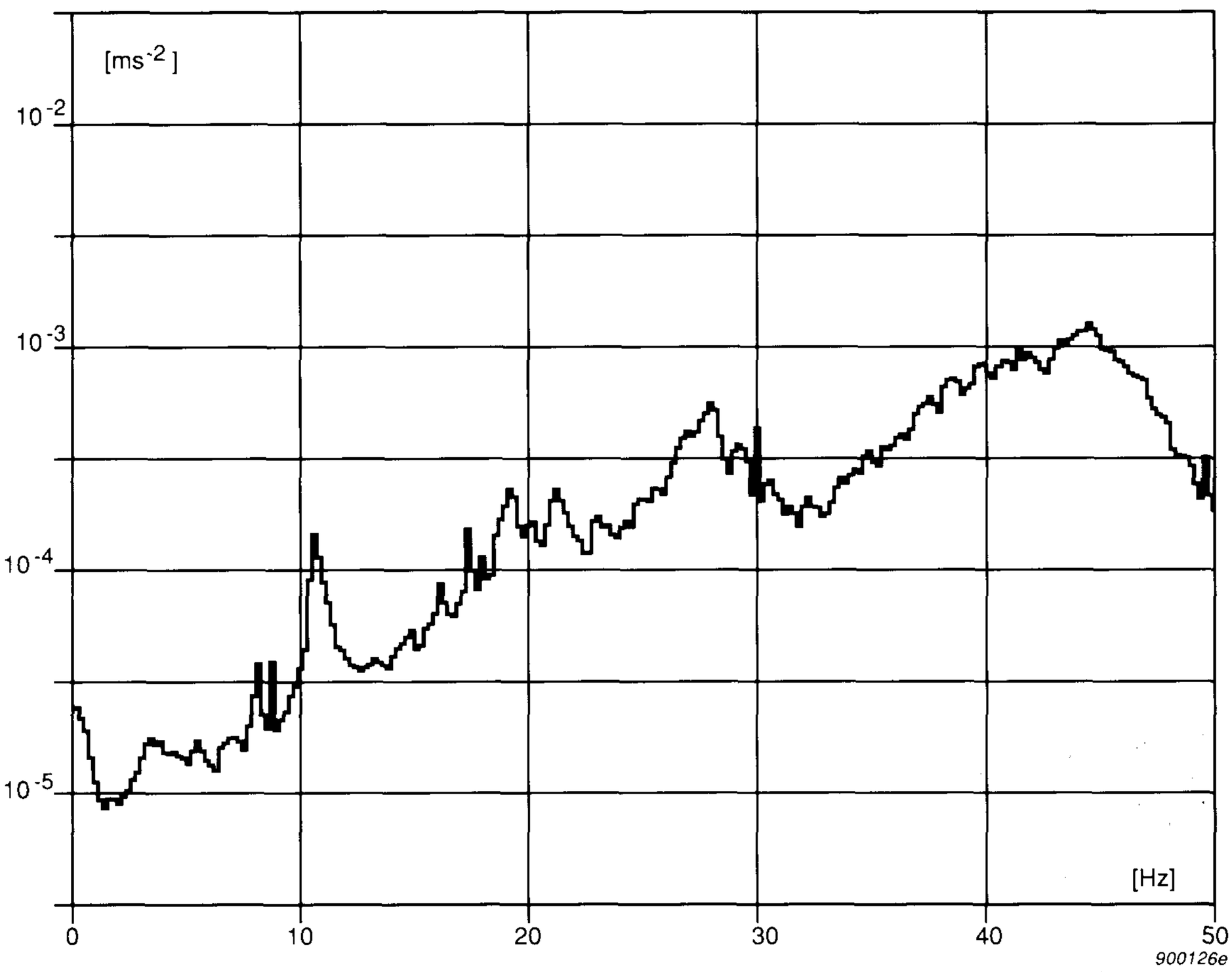

Fig. 14. Low frequency RMS vibration spectrum measured on an office desk

mised. This was another good reason for designing a dedicated PAS microphone/preamplifier unit.

The physical deformation of the cell due to vibration causes a modulation of the cell volume which gives rise to a vibration signal with the same phase for both microphones. This contribution can, therefore, not be cancelled. Fortunately, it is much smaller than p_m and p_{air}.

Finally, if vibration of the cell is rotational, not linear, it will create small signals with equal phase and therefore the vibration signals will not be balanced-out, but added. However, this signal is also much smaller than p_m and p_{air}.

Fig. 14 shows a typical low frequency vibration spectrum as measured on a table in an office environment, using a bandwith of 1/8 Hz, and averaged over a period of time. At 20 Hz, as read from the curve, the vibration level is $1{,}7 \cdot 10^{-4}\,ms^{-2}$, causing a vibration signal = $p_m + p_{air} = 6{,}3 \cdot 10^{-6}$ Pa. When adding the microphone signals, a residual vibration signal is left, which is due to (1) imperfect balancing-out of p_m and p_{air}, (2) rotational vibration, and (3) deformation of the cell. In practice an improvement factor of 50 is typically obtained which makes the residual vibration signal equal to $1{,}3 \cdot 10^{-7}$ Pa. This is 40 times lower than the detection limit and therefore, in such an environment, vibration will not compromise the detection limit. In a vibrationally harsh environment, however, some care should be taken in the mounting of the 1302/1306.

e. The dust signal

Small particles of any kind, when present in the PAS cell, will absorb part of the light energy, and thus cause a disturbing signal, a dust signal. Dust particles are almost always present in the environment and they are drawn into the PAS cell with the air. A $10\,\mu m$ dust filter prevents the bigger particles from passing into the cell.

In order to estimate the size of the dust signal, we suppose that all the dust particles are identical, spherical in shape, have a diameter d and that the basic dust material has a mass density ρ_{dust}. We will also assume that the dust is optically black. Using this simple model, the dust can be characterized by an absorption coefficient:

$$k_{dust} = \frac{3}{2\,\rho_{dust}\,d} \tag{31}$$

As long as dust concentrations are not extremely high, we can neglect the heat capacity of the dust particles when calculating the acoustic signal produced by the absorbed light energy. This implies that we can use the detection-limit equation (24) to calculate the dust detection limit by inserting k_{dust} from equation (31):

$$\text{Detection Limit} = \frac{\rho_{\text{dust}}\ d \cdot 3 \cdot 10^{-3}\ [\text{Wm}^{-3}\,\text{sr}^{-1}]}{T_f L_\nu\ \Delta\nu} \tag{32}$$

Using optical filter UA 0984, and assuming $\rho_{\text{dust}} = 2 \cdot 10^3\ \text{kg/m}^3$, the detection limit is found to be 0,04 · d, which with a 10 μm particle diameter gives a detection limit of 400 $\mu\text{g/m}^3$. According to the formula, the detection limit is proportional to the particle diameter d, which implies that smaller particles cause a higher dust signal. In normal living areas, the typical concentration of dust particles with a diameter less than 10 μm is of the order of 50 $\mu\text{g/m}^3$, which gives a resultant dust signal 8 times less than the dectection limit. This is a worst case calculation as we are assuming that we have optically black dust. This assumption is conservative especially when the dust particles have a diameter which is close to, or smaller than, the wavelength of the light. Therefore, in this kind of dust environment the dust signal does not create any problem.

f. Microphone/preamplifier noise

The PAS system microphones are ½ inch low noise electret microphones with built in preamplifiers, which have been optimized in several ways for use with a PAS system.

The signals from the two microphones are added, which doubles the gas signal while only increasing the random noise by 3 dB. This results in a 3 dB improvement in the signal to noise ratio. Fig. 15 shows the low frequency equivalent noise spectrum, due to electronic noise in the preamplifier, as measured on the summed output using a bandwidth of ⅛ Hz. Notice that the noise level is more or less constant at higher frequencies, but increases at lower frequencies. Thus, by going from 20 Hz to 10 Hz, the noise increases 4 dB, compared to an increase of the photoacoustic gas signal of 5,4 dB (see Fig. 13) i.e. the improvement in signal to noise ratio thus obtained is insignificant.

At 20 Hz, the RMS noise level corresponding to the actual bandwidth and averaging time used in the 1302 and 1306 is in accordance with a mea-

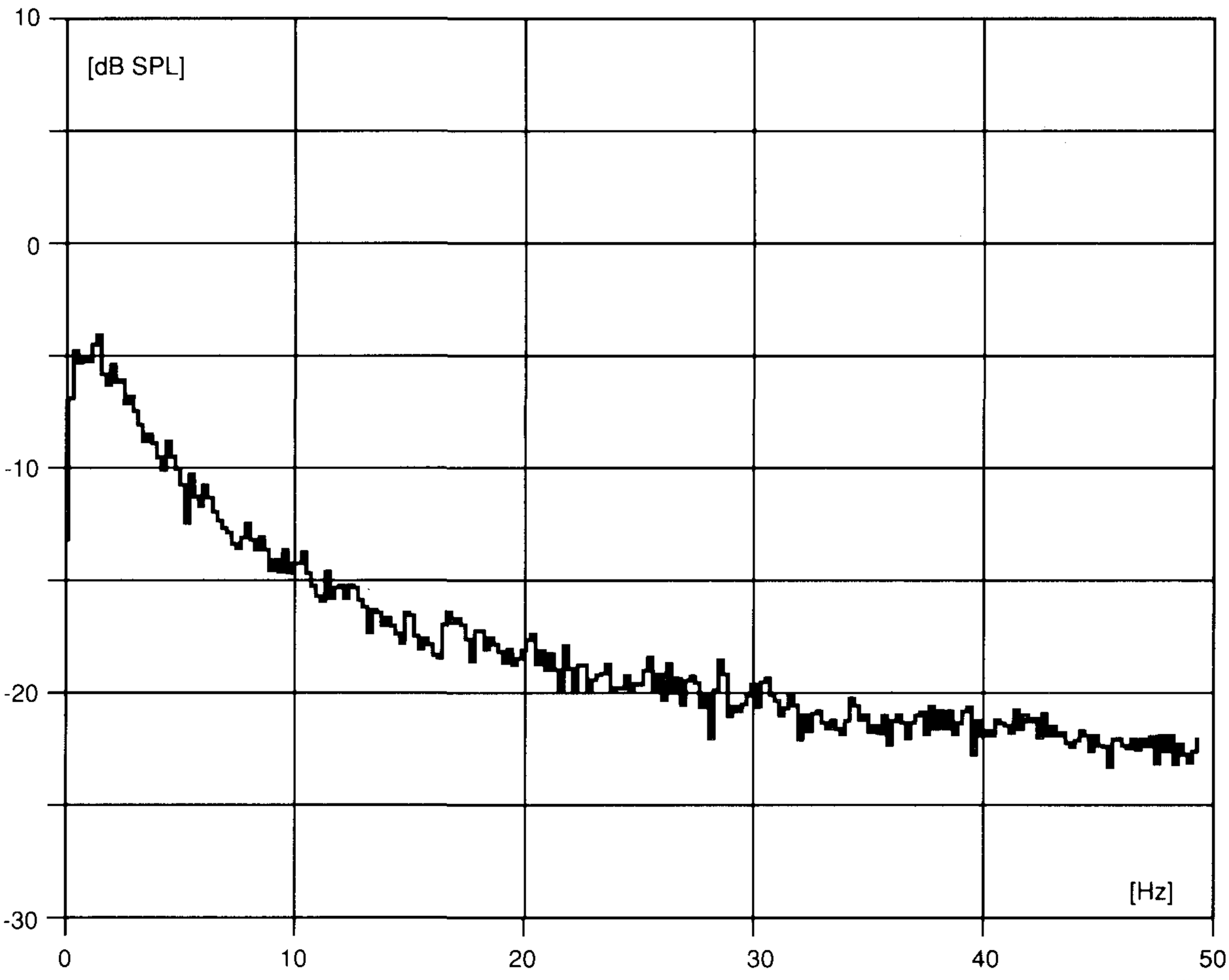

Fig. 15. Low frequency RMS preamplifier noise spectrum

surement equal to $2{,}5 \cdot 10^{-6}$ Pa. The detection limit signal, defined as the signal equal to twice the RMS noise level, thus corresponds to a sound pressure of $5 \cdot 10^{-6}$ Pa.

6. Absorption in non-polluted atmospheric air

The composition of dry, non-polluted atmospheric air is approximately: 78% nitrogen, 21% oxygen, 0,9% argon, 340 ppm carbon dioxide, 1,5 ppm methane, 0,3 ppm nitrous oxide, plus trace concentrations of the noble gases. Normal atmospheric air also contains a varying amount of water vapour, typically in the range of 10 000 – 20 000 ppm.

When measuring trace amounts of toxic gases present in atmospheric air, gases normally present in atmospheric air have the potential of interfering with the measurement. Two gases which are present in the highest concentrations, that is, nitrogen and oxygen, are homopolar molecules,

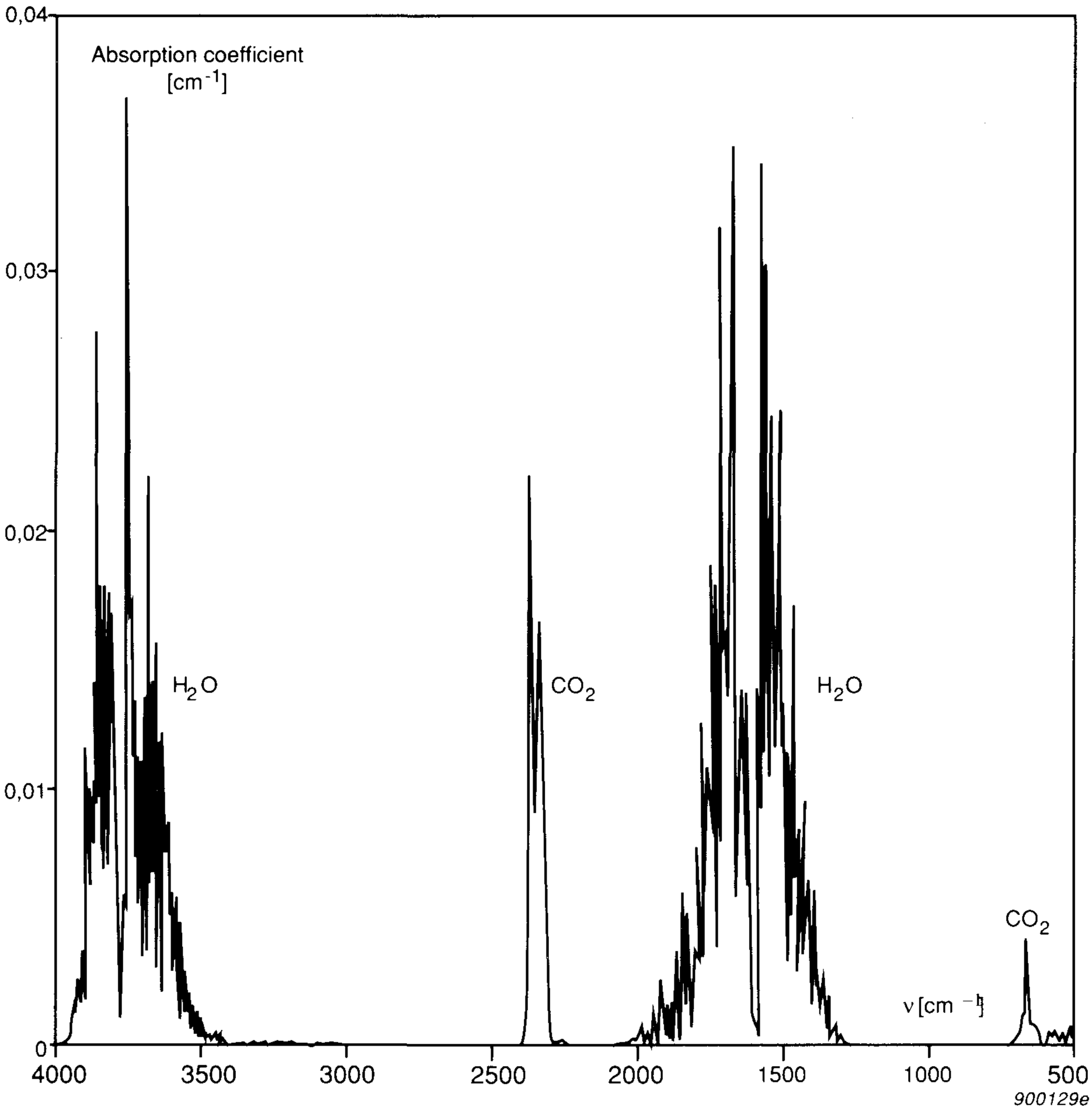

Fig. 16. The infra-red absorption spectrum of atmospheric air with 20000 ppm water vapour and 340 ppm carbon dioxide (resolution: 10 cm^{-1})

which fortunately do not absorb infrared light. Neither does argon, nor the other noble gases, as they exist as single atoms. In atmospheric air, water vapour and carbon dioxide are the strongest absorbers and methane and nitrous oxide are the weaker absorbers.

Fig. 16 shows the absorption spectrum of atmospheric air containing 20000 ppm water plus 340 ppm carbon dioxide. It shows two major frequency ranges with low absorption: 2400 – 2800 cm^{-1} and 800 – 1200 cm^{-1},

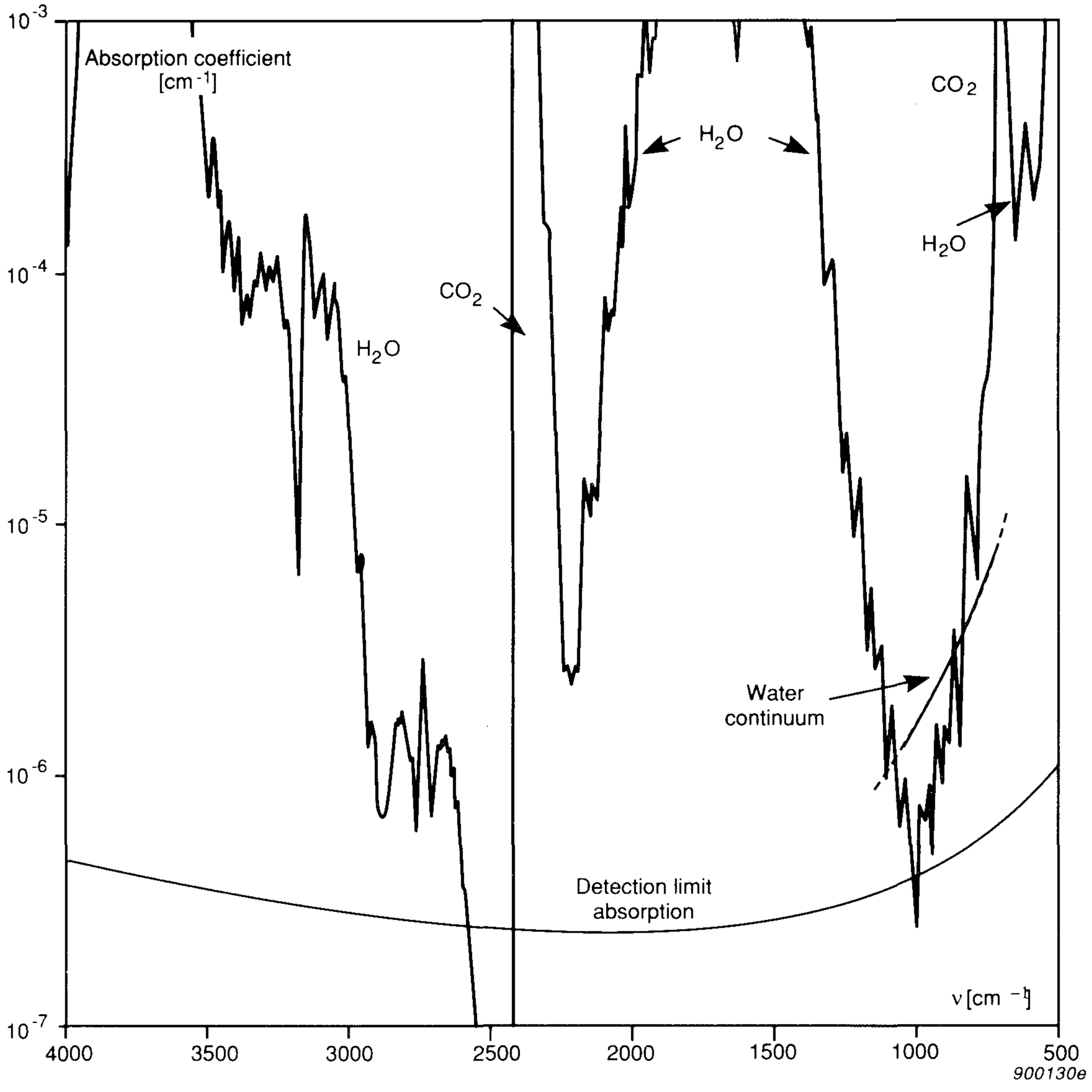

Fig. 17. Illustration showing (a) the infra-red absorption spectrum of atmospheric air in the low-absorption ranges (resolution: 20 cm^{-1}); and (b) the water continuum absorption; and (c) the detection limit absorption

plus a narrow range around 2200 cm^{-1}. The two major low absorption ranges are often referred to as "the atmospheric windows".

Fig. 17 shows the same absorption spectrum as Fig. 16, but on a logarithmic scale in order to enhance the absorption in the frequency ranges where the absorption is low. The spectrum is averaged over a bandwidth of 20 cm^{-1}.

Fig. 17 further shows the so-called water continuum absorption at a concentration of 20 000 ppm. As the name indicates, the water continuum absorption is due to water vapour absorption, as is the water spectral absorption. What is the difference then?

The origin of the water continuum absorption is, at least for the major part, due to the extreme wings of the strong water spectral lines at long wavelengths. It exhibits no spectral structure as does the spectral absorption, and while the spectral water absorption is proportional to the concentration of the water vapour, the continuum absorption is approximately proportional to the square of the concentration at concentration levels which are typical in atmospheric air. In the major part of the 800 cm^{-1} to 1200 cm^{-1} atmospheric window, from Fig. 17, the contribution due to the continuum water absorption dominates over the spectral contribution. At higher frequencies, the continuum absorption becomes small.

Fig. 17 finally shows the average absorption coefficient at the detection limit, using a hypothetical optical filter with a bandwidth of 60 cm^{-1} and a peak transmission of 50%: these values are quite typical for a majority of the available optical filters. The frequency dependence of this curve is due to the frequency dependence of the L_ν curve, as the detection limit is inversely proportional to L_ν. As is evident from Fig. 17, the detection limit, even in the major part of the atmospheric windows, is smaller than the water absorption. Therefore, if water interference was not compensated for, it would limit the performance of the PAS system when gases are measured in atmospheric air. In 1302 and 1306, however, the water concentration is monitored with the purpose of compensating the photoacoustic signal for the water vapour contribution. As with the zero-air signal, the water signal's dependence on the water concentration and temperature has been carefully mapped for each of the available optical filters. Thus, after a humidity-interference calibration, in which humidified zero-air is measured, the instrument can automatically compensate for water vapour interference in the air mixture being measured, at various temperatures and water-vapour concentrations.

7. Introduction to interference and linearity

Interference

The 1306 contains only one (interchangeable) optical filter, and is intended for outdoor monitoring of a single gas or a group of gases, for the pur-

pose, for instance, of detecting accidental gas releases. The 1302, however, can be equipped with up to five different filters thus making it possible to monitor 5 different gases at a time. Assume, for example, that we wish to monitor halothan and enflurane (which are both anesthetic gases) at the same time. By studying their absorption spectra (see Fig. 18) one can see that it is difficult to select an appropriate absorption band where it is possible to measure one of the gases without being disturbed by interference from the other, and vice versa. However, it is still possible to measure each of the gases correctly because the signals measured with each of the two optical filters contains information about both gases present. This feature is called cross compensation, and it works with up to five different gases, even if they have overlapping spectra. Cross compensation reduces the effect of interference to such an extent, that in many cases it can be com-

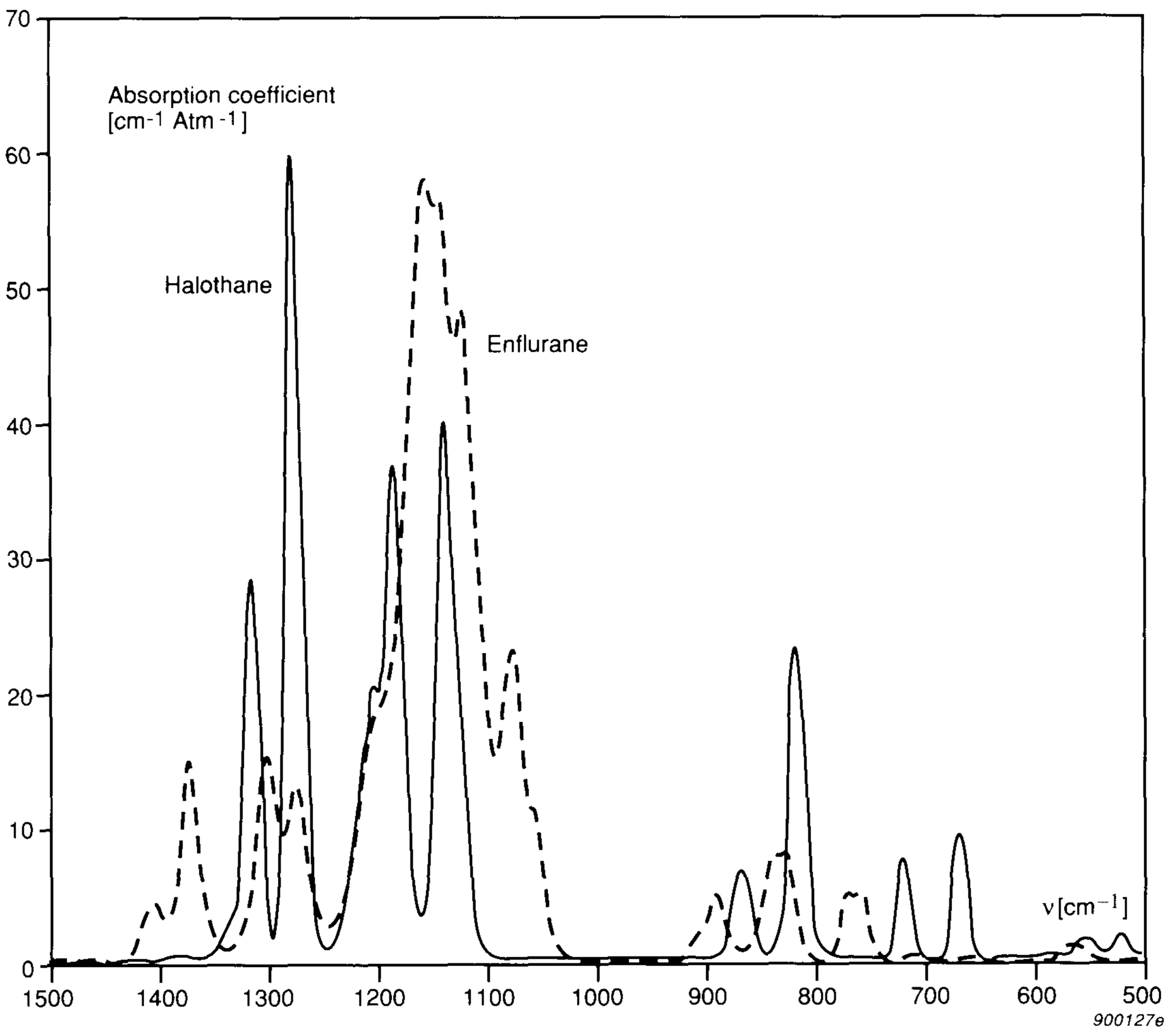

Fig. 18. Absorption spectra of enflurane and halothane (resolution: 5cm^{-1})

pletely neglected. It is the cross compensation feature of the 1302, — not the selectivity of the individual optical filters — that is the fundamental basis for the selectivity of the 1302 for a limited number of known gases.

Linearity

The linearity range of 1302/1306 depends to some extent on the detailed structure of the absorption band being utilized, and to some extent on which optical filter is used. Generally speaking, the linear range will typically extend to a factor of 10 000 above the detection limit.

The linearity range can be even further extended by compensating for non-linearity. In 1302, this compensation is a built-in feature which uses a unique compensation algorithm. It simply requires a two-point span calibration to be performed, i.e. measuring, in turn, two different concentrations of a gas — where the low concentration preferably lies within the linear range, and the high concentration lies close to the upper limit of the non-linear range. In this way, the dynamic range can be extended to some 5–6 decades (a factor of 100 000–1 000 000 above the detection limit).

8. Discussion

We have discussed the advantages and limitations of the PAS technique in a fairly simple fashion, which in no way gives full credit to the time and resources used in developing the technique during the past 5–10 years. Dozens of man-years have been used in "fine-tuning" our PAS instruments to give the absolute maximum performance.

As we have discussed, if we assume that the wall- and water signals have been compensated for, the sensitivity of the Brüel & Kjær PAS system is only limited by the microphone/preamplifier noise with most of the optical filters.

Suppose that, in one way or another, it was possible to reduce the microphone/preamplifier noise, or, alternatively, increase the gas signal by increasing the amount of light energy entering the PAS cell, would the PAS system then be better suited to its purpose?

The wall- and water signal compensation would then be more critical, and this would make it difficult to obtain a stable zero signal when the ambient humidity and temperature varied. This problem could, however, be solved if it was possible to dry the air sample without affecting the concentration of the gas to be measured. The wall signal could be decreased by increasing the size of the PAS cell, as it is inversely related to

the cell's linear dimensions. This would require a correspondingly bigger and more power-consuming black body infrared source — its power consumption being largely proportional to the square of its linear dimensions.

Increasing the size of the PAS cell would result in an increased vibration signal. Environmental vibration would then become a limiting factor in many measuring situations. This could, however, be overcome by suitably isolating the PAS system from vibrations in its environment, but in practice isolating the system from vibrations as low as 20 Hz is not very straightforward.

As it can be seen, it is theoretically possible to improve the Brüel & Kjær PAS system, but at the cost of significantly increasing the complexity of the system, its bulk, its power consumption and its price. We believe that the performance of the small, light-weight, fully self-contained PAS instruments developed by Brüel & Kjær is close to optimal.

References

[1] Rosencwaig, A.: "*Photoacoustics and Photoacoustic Spectroscopy*". John Wiley & Sons, 1980.

[2] Pao, Yoh-Han: "*Optoacoustic Spectroscopy and Detection*". Academic Press, 1977.

[3] Brüel & Kjær: "*Photoacoustics in Gas Detection*".

[4] Brittain, E.F.H., George, W.O., Wells, C.H.J.: "*Introduction to Molecular Spectroscopy. Theory and Experiment*". Academic Press, 1970.

[5] Rothman, L.S., *et al*: "*AFGL Atmospheric Absorption Line Parameters Compilation: 1982 Edition*". Applied Optics, Vol. 22, No. 15, 1983.

[6] Burch, D.E., Alt, R.L.: "*Continuum Absorption by H_2O in the 700 – 1200 cm^{-1} and 2400 – 2800 cm^{-1} Windows*". AFGL–TR–84–0128, 1984.

[7] Stokkebro Hansen, J., Christensen, D.H., and Nicolaisen, F.M.: "*Infrarøde gasspektre (4000 – 380 cm^{-1}) af 50 stoffer med henblik på kvantitativ bestemmelse i atmosfærisk luft*". Internal Report, August 1983, Kemisk Laboratorium 5, H.C. Ørsted Institutet, Københavns Universitet.

Previously issued numbers of Brüel & Kjær Technical Review

(Continued from cover page 2)

3–1984 The Hilbert Transform
Microphone System for Extremely Low Sound Levels
Averaging Times of Level Recorder 2317
2–1984 Dual Channel FFT Analysis (Part II)
1–1984 Dual Channel FFT Analysis (Part I)
4–1983 Sound Level Meters – The Atlantic Divide
Design principles for Integrating Sound Level Meters
3–1983 Fourier Analysis of Surface Roughness
2–1983 System Analysis and Time Delay Spectrometry (Part II)
1–1983 System Analysis and Time Delay Spectrometry (Part I)
4–1982 Sound Intensity (Part II Instrumentation and Applications)
Flutter Compensation of Tape Recorded Signals for Narrow Band Analysis
3–1982 Sound Intensity (Part I Theory).
2–1982 Thermal Comfort.
1–1982 Human Body Vibration Exposure and its Measurement.
4–1981 Low Frequency Calibration of Acoustical Measurement Systems.
Calibration and Standards. Vibration and Shock Measurements.
3–1981 Cepstrum Analysis.
2–1981 Acoustic Emission Source Location in Theory and in Practice.
1–1981 The Fundamentals of Industrial Balancing Machines and Their Applications.
4–1980 Selection and Use of Microphones for Engine and Aircraft Noise Measurements.
3–1980 Power Based Measurements of Sound Insulation.
Acoustical Measurement of Auditory Tube Opening.
2–1980 Zoom-FFT.

Special technical literature

Brüel & Kjær publishes a variety of technical literature which can be obtained from your local Brüel & Kjær representative.
The following literature is presently available:

- ○ Mechanical Vibration and Shock Measurements (English), 2nd edition
- ○ Modal Analysis of Large Structures–Multiple Exciter Systems (English)
- ○ Noise Control (English, French)
- ○ Frequency Analysis (English)
- ○ Catalogues (several languages)
- ○ Product Data Sheets (English, German, French, Russian)

Furthermore, back copies of the Technical Review can be supplied as shown in the list above. Older issues may be obtained provided they are still in stock.

Brüel & Kjær

WORLD HEADQUARTERS: DK-2850 Nærum · Denmark
Telephone: +45 42 80 05 00 · Telex: 37316 bruka dk · Fax: +45 42 80 14 05 / +45 42 80 21 63

Australia (02) 450-2066 · Austria 02235/7550*0 · Belgium 02 · 242-97 45 · Brazil (011) 246-8149/246-8166
Canada (514) 695-8225 · Finland (90) 80 17 044 · France (1) 64 57 20 10 · Federal Republic of Germany 04106/70 95-0
Great Britain (01) 954-2366 · Holland 03402-39994 · Hong Kong 5487486 · Hungary (1) 133 83 05/133 89 29
Italy (02) 52 44 141 · Japan 03-438-0761 · Republic of Korea (02) 554-0605 · Norway 02-90 44 10
Portugal (1) 65 92 56/65 92 80 · Singapore 225 8533 · Spain (91) 268 10 00 · Sweden (08) 711 27 30
Switzerland (042) 65 11 61 · Taiwan (02) 713 9303 · USA (508) 481-7000
Local representatives and service organisations world-wide

ISSN 007–2621

BV 0041–11

PRINTED IN DENMARK BY NÆRUM OFFSET